NATIONAL ADVISORY COMMITTEE FOR AERONAUTICS

TECHNICAL NOTE

No. 1211

THE FLOW AND FORCE CHARACTERISTICS OF SUPERSONIC AIRFOILS AT HIGH SUBSONIC SPEEDS

By W. F. Lindsey, Bernard N. Daley, and Milton D. Humphreys

Langley Memorial Aeronautical Laboratory
Langley Field, Va.

Washington
March 1947

NATIONAL ADVISORY COMMITTEE FOR AERONAUTICS

TECHNICAL NOTE NO. 1211

THE FLOW AND FORCE CHARACTERISTICS OF SUPERSONIC AIRFOILS AT HIGH SUBSONIC SPEEDS

By W. F. Lindsey, Bernard N. Daley,
and Milton D. Humphreys

SUMMARY

An investigation has been conducted at subsonic Mach numbers in the Langley rectangular high-speed tunnel on five supersonic airfoils and, for comparison, on two subsonic airfoils. Two-dimensional data were obtained by pressure measurements and schlieren photographs at angles of attack from 0° to 4° for Mach numbers between 0.30 and 0.90 for these 6-percent-thick symmetrical airfoils.

The results indicated that the drag coefficients are generally higher at subsonic Mach numbers for the supersonic airfoils than for the subsonic airfoils, but the normal-force and pitching-moment characteristics of those supersonic airfoils having their maximum thickness located at the 0.7-chord station would diminish the problems generally encountered in longitudinal control at high Mach numbers.

The investigation also revealed the occurrence of an unusual flow phenomenon at the leading edge of the supersonic airfoils at the higher Mach numbers. This phenomenon, through the elimination of an extensive separated-flow condition over the forward part of the airfoil, effected a rather sudden increase in normal-force coefficient and in some cases a decrease in the drag coefficient.

INTRODUCTION

In the design of supersonic aircraft, the amount of sweepback incorporated in the lifting surfaces could affect the choice of the type of profile for those surfaces. If the component of stream velocity normal to the leading edge of the lifting surface is subsonic, a rounded leading edge or subsonic airfoil might be used. On the other hand, if the normal component of the stream velocity is supersonic, a sharp leading edge or supersonic airfoil is definitely needed to minimize the wave resistance. Since consideration of the

structural and stability requirements may limit the amount of sweep, the velocity normal to the leading edge may necessarily be supersonic and sharp-edge airfoils are then required. The lifting surfaces of supersonic airplanes and other bodies therefore might be expected to have sharp leading edges. For some flight conditions these lifting surfaces must necessarily operate at subsonic speeds. In order to provide information important in the selection of airfoils for supersonic aircraft the aerodynamic characteristics of thin, sharp-edge airfoils therefore must be determined at subsonic Mach numbers.

The available results of previous investigations at subsonic Mach numbers on airfoils having sharp leading edges have been limited to two 9-percent-thick models, a part of a subsonic-airfoil-development investigation (reference 1), and to earlier exploratory tests on two 8-percent-thick models (reference 2).

Because of the limited data available and the need for even thinner profiles than those previously tested for high-speed applications, an investigation has been conducted in the Langley rectangular high-speed tunnel on five supersonic-type airfoils and, for comparison, on two subsonic-type airfoils. All airfoil models were symmetrical and of 6-percent maximum thickness. Test data were obtained by means of static-pressure measurements along the surfaces of the airfoils, total pressure surveys in the wake, and schlieren photographs of the flow at Mach numbers up to 0.90.

SUPERSONIC-AIRFOIL PROFILE DESIGNATION

Theory and experiment have shown that at supersonic speeds airfoils of simple geometric shape are quite efficient. The two airfoil shapes most commonly encountered are the double-wedge or diamond profile and the profile formed by a combination of two or more circular arcs. Since both double-wedge and circular-arc profiles can represent a series of forms, neither of these profiles is specifically defined by giving the general shape without additional detailed information.

With the bow wave attached to the leading edge of an airfoil in a supersonic flow, the flow over one surface is not affected by the flow over the other surface. Consequently, the profile can be considered to be composed of two parts, one on either side of the chord (line joining leading and trailing edges). Thus, if the maximum thickness of each surface and the chordwise location of the maximum thickness are given, the thickness and camber are specified.

The combination of the general shape, the maximum thickness, and the chordwise location of maximum thickness for each surface specifically defines the profile. The following general form for designating the supersonic airfoils has been adopted:

$$\text{NACA NS-}(X_1)(Y_1)\text{-}(X_2)(Y_2)$$

In the actual designation, the letter "N" is replaced by the series number, the number "1" being used for the diamond- or wedge-shape profiles and the number "2" being used for the circular-arc profiles. The letter "S" denotes supersonic. The letter "X_1" represents the distance along the chord from the leading edge to the point of maximum thickness "Y_1" for the upper surface. The letters "X_2" and "Y_2" represent the corresponding values for the lower surface. Numerical values substituted for the X's and Y's are in percent chord. (See fig. 1.) The following is a sample designation:

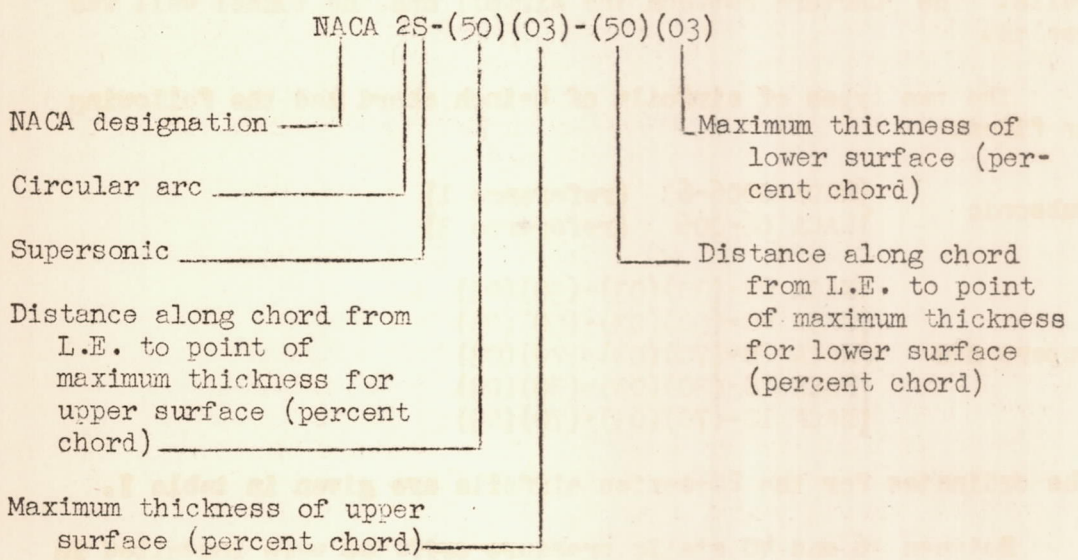

In case the maximum thickness for the lower surface Y_2 is constant for a distance along the chord, the numerical substitution for X_2 should be compounded to include the two values limiting the range of constant thickness. Thus, if the airfoil given in the sample designation were cambered by making the lower surface coincide with the chord and the thickness of the upper surface were retained at 3 percent, the designation would be

$$\text{NACA 2S-(50)(03)-(0-100)(00)}$$

APPARATUS AND TESTS

The tests were conducted in the Langley rectangular high-speed tunnel, which is an induction-type tunnel without return passages and has an 18-inch by 4-inch test section. The variation in Mach number in the test section along the tunnel axis without a model installed in the tunnel is ±0.4 percent of the stream Mach number. In a plane normal to the tunnel axis, the variation is ±1 percent of the stream Mach number. The air flow for this investigation appears to be slightly misalined with a possible variation of ±0.1°. The geometric angles of attack are accurate to ±0.05°.

Each airfoil completely spanned the test section along the 4-inch dimension and was supported by large circular end plates, which were fitted into the tunnel walls in such a way as to rotate with the model and to retain continuity of the surface of the tunnel walls. The juncture between the airfoil and the tunnel wall was sealed.

The two types of airfoils of 4-inch chord had the following profiles:

Subsonic	NACA 0006-63 (reference 1) NACA 66-006 (reference 3)
Supersonic	NACA 2S-(30)(03)-(30)(03) NACA 2S-(50)(03)-(50)(03) NACA 2S-(70)(03)-(70)(03) NACA 1S-(30)(03)-(30)(03) NACA 1S-(70)(03)-(70)(03)

The ordinates for the 2S-series airfoils are given in table I.

Between 36 and 40 static pressure orifices were installed in the model surfaces of each airfoil in two chordwise rows 1/4 inch from and on either side of the model center line. The number of orifices installed depended on the thickness distribution and hence was a minimum for the 1S-series airfoils. The static-pressure-orifice locations are shown on the profiles in figure 1. The absence of pressure orifices at the leading and trailing edges of the airfoils resulted from a physical limitation on the installation of orifices and pressure ducts.

Pressure-distribution measurements and wake surveys were made for Mach numbers between 0.30 and 0.90 at angles of attack of 0° to 4°. This Mach number range corresponded approximately to a

Reynolds number range from 0.7 to 1.5×10^6. Additional data were obtained in the form of schlieren photographs of the flow. These photographs show density gradients in the flow by changes in light intensity. Supplementary tests were made by measuring the static pressures on the wall in the vicinity of the intersection of the model with the tunnel wall to provide some information on the conditions within the flow field near the leading edge of the 1S-type airfoils.

SYMBOLS

M	stream Mach number
M_f	Mach number in flow field
M_{ch}	stream Mach number at choking
M_l	local Mach number at surface
q	dynamic pressure
p	stream static pressure
p_l	local static pressure at model surface
P	pressure coefficient $\left(\frac{p_l - p}{q}\right)$
P_{cr}	critical pressure coefficient $\left(\frac{0.528\ H - p}{q}\right)$
H	stream total pressure
c_n	section normal force coefficient
$c_{m_{c/4}}$	section pitching-moment coefficient of normal force about quarter-chord location
c_d	section drag coefficient (determined from wake surveys)
α	angle of attack
c	airfoil chord

TUNNEL-WALL EFFECTS

The data obtained from this investigation are subject to a correction because of tunnel-wall effects. The theoretically derived correction (reference 4) indicates generally that, for a given ratio of model chord to tunnel height, the error increases with Mach number and drag coefficient. The error is also affected to some extent by the type of profile. The ratio of the corrected values to the uncorrected values were determined by the method of reference 4 for these data at several Mach numbers and at an angle of attack of 4° (a high drag-coefficient condition). These ratios, wherein the corrected values are indicated by the primed symbols, are:

M	M'/M	c_n'/c_n	c_d'/c_d	$c_{m_{c/4}}'-c_{m_{c/4}}$	$\alpha' - \alpha$
0.60	1.005±0.001	0.978±0.002	0.990±0.002	0.002±0.000	0.059±0.007
.70	1.007± .001	.970± .001	.986± .002	.002± .001	.073± .009
.80	1.018± .004	.951± .004	.973± .004	.005± .002	.090± .015

In the preceding table the variations in the correction for a given condition are due to a combination of differences in drag coefficient and shape of profile for the seven airfoils investigated. The variations can be seen to be quite small and hence would not affect a comparison of the relative merits of the two types of airfoils.

An examination of the correction for Mach numbers and aerodynamic coefficients shows that the principal effect of these corrections would be to reduce somewhat the variation of the coefficient with Mach number for all the airfoils in the higher speed range. Although the methods of correcting the force and moment coefficients, angle of attack, and Mach number are not too difficult, no comparable methods exist for correcting the pressure-distribution diagrams. A correction for the pressure-distribution diagram would involve not only dynamic pressure, Mach number, and angle of attack, but also the distribution along the chord. Thus, the application of the correction would be quite involved and at the higher Mach numbers could be subject to question. Inasmuch as the corrections would have no significant effect on the conclusions to be drawn from this investigation and since all of the data could not be comparably corrected, the data are presented uncorrected.

At the choking Mach number where sonic velocities extend from model to tunnel walls, the static pressure is lower behind the model than ahead of the model. Large static pressure gradients are thus produced in the flow at the choking Mach number, and data

obtained at that Mach number are of questionable value. The data at and within 0.025 and 0.030 of the choking Mach number are indicated on the figures in which they appear by dotted lines or other notations.

RESULTS

The effect of angle of attack and Mach number on the pressure distributions for the seven airfoils investigated is shown in figure 2. The section normal force and pitching moment of the normal force about the quarter-chord point have been obtained from integration of pressure-distribution diagrams and are presented in coefficient form in figures 3 to 5. The drag-coefficient data obtained from wake surveys are presented in figures 6 and 7. Data from figures 3 and 6 are cross-plotted in figure 8 to show the variation of drag coefficient with normal-force coefficient at a constant Mach number for the various profiles.

The development of an unusual flow phenomenon as the Mach number is increased for a fixed angle of attack is shown in figure 9 for the NACA 1S-(70)(03)-(70)(03) airfoil. Figure 10 shows the phenomenon on all supersonic profiles tested at a constant angle of attack and Mach number. The variation of the phenomenon with angle of attack on a given profile is shown in figure 11. Measurements in the flow field are presented and compared with flow photographs and local Mach number distributions in figure 12. The effect of large changes in leading-edge shape on the phenomenon is shown in figure 13.

DISCUSSION

Pressure distribution.- An examination of the pressure-distribution diagrams for the airfoils investigated (fig. 2) did not reveal any marked differences in the effect of compressibility on the flow past the subsonic and supersonic airfoils, with the exception of a somewhat more irregular distribution of pressures along the chord for the supersonic airfoils, especially at an angle of attack of 4°.

The determination of the pressures near the leading edge of the airfoils was hindered, however, by a physical limitation on pressure orifice installation. Information obtained from the measurements of pressure in the flow field indicated that the pressures near the leading edge on the upper surface might be appreciably lower than the faired values shown in figure 2, as illustrated by the local Mach

number distribution shown at a Mach number of 0.8 in figure 12(a). As a result of this probable error in the fairing of the pressure diagrams at the leading edge of the airfoils at angles of attack greater than 0°, the critical Mach number could not be accurately determined, and in addition, the normal-force coefficients may be expected to be higher than those presented herein.

Normal-force coefficients.- The variation of the section normal-force coefficient c_n with Mach number M (fig. 3) at angles of attack of 2° and 4° generally appeared to be less throughout the Mach number range investigated for the supersonic airfoils than for the subsonic airfoils. The reduced effect of compressibility on the variation of c_n with α as shown in figure 4(a) tends to minimize the problems associated with longitudinal control at high Mach numbers.

In addition, the effect of α on c_n at angles between 0° and 2° (fig. 4(b)) was generally less for the supersonic airfoils than for subsonic airfoils; this effect was probably the result of early separation from the sharp leading edges and could have been predicted from low-speed considerations. The effect of α on c_n at angles between 2° and 4° for supersonic airfoils, however, was greater in general than for the lower α range, especially for those airfoils having maximum thickness locations at or behind the 0.5c station. The one exception to these generalizations was the NACA 1S-(30)(03)-(30)(03) airfoil, which had normal-force characteristics comparable with those of the subsonic airfoils (fig. 4(b)).

The normal-force characteristics of the supersonic airfoils presented herein indicated that the problems associated with the subsonic flight of supersonic aircraft would not be aggravated by use of these airfoils; in fact, some problems associated with longitudinal control might be minimized.

Pitching-moment of normal-force about quarter-chord point.- The variation of the section pitching-moment coefficient $c_{m_{c/4}}$ with stream Mach number for the subsonic airfoils (figs. 5(a) and 5(b)) was small at Mach numbers below 0.70, whereas at Mach numbers of 0.80 and above the variation had a large negative trend. The variation of $c_{m_{c/4}}$ with α is shown to be small in the lower Mach number range, but at Mach numbers above 0.80, an appreciable negative trend is indicated.

The supersonic airfoils also showed only a small effect of both M and α on $c_{m_{c/4}}$ at Mach numbers below 0.70 (figs. 5(c) to 5(g)). At Mach numbers greater than 0.80, however, the variation of $c_{m_{c/4}}$ with M for the supersonic airfoils showed a definite effect of maximum-thickness location. Those airfoils having maximum thickness located at 0.3c (figs. 5(c) and 5(f)) as well as both airfoils of the subsonic type (figs. 5(a) and 5(b)) had a negative slope of $c_{m_{c/4}}$ with α at Mach numbers greater than 0.80. Shifting the maximum-thickness location to the 0.7 chord station (figs. 5(e) and 5(g)) resulted at the high Mach numbers in a small positive slope of $c_{m_{c/4}}$ with α that could be desirable for longitudinal control at high speeds.

Drag coefficient.- The general effects of compressibility on the drag coefficients of both supersonic- and subsonic-type 6-percent-thick airfoils (fig. 6) are in accord. There are, however, a few differences that are best shown in the comparison between airfoils at each of two angles of attack in figure 7. At an angle of attack of 0° (fig. 7(a)) and a Mach number of 0.5, a gradual rise is noted in drag coefficient from a minimum for the NACA 2S-(50)(03)-(50)(03) airfoil to the highest values for the 1S-series.

At an angle of attack of 0° little difference is indicated in the Mach number at which the drag break occurs for the two subsonic-type airfoils, and the NACA 2S-(70)(03)-(70)(03) and NACA 2S-(50)(03)-(50)(03) airfoils. The obviously earlier drag break for the two airfoils of the 1S-series results from the high induced velocities (fig. 2) and is of the type associated with flow separations which could have been expected to occur at the abrupt (8.2°) change in surface slope at the maximum-thickness location.

The drag coefficient for the various airfoils at an angle of attack of 4° (fig. 7(b)) for Mach numbers between 0.5 and 0.6 is indicative of the extent of flow separation from a minimum for the NACA 0006-63 to a maximum for the NACA 1S-(70)(03)-(70)(03). The gradual rise in drag coefficient between Mach numbers of 0.6 and 0.7 for the NACA 0006-63 airfoil is indicative of a condition of progressively increasing extent of separated flow.

The drag normal-force relations for the various profiles and the effect of compressibility on that relation (fig. 8) provides a better basis of comparison of the drag characteristics than figure 7. The results of figure 8 indicated that within the range of the investigation, the drag for a given normal force is generally higher

for the supersonic type airfoils than for the subsonic type. The differences are not so large that functioning of supersonic aircraft would be excessively affected at subsonic speeds.

There is some indication in figure 8 that, at the higher Mach numbers, and at high values of normal-force coefficient, the value of drag coefficient might be less for some of the supersonic airfoils than for the subsonic airfoils. As a result of this indication, the original investigation is being extended to determine the characteristics of these profiles at high angles of attack.

Unusual flow at high Mach numbers.- During this investigation an unusual type of flow phenomenon was observed to occur at the higher Mach numbers in the vicinity of the leading edge of the supersonic airfoils under lifting conditions. The development of this phenomenon with increasing Mach number and the changes in the flow that accompany it are shown by the schlieren photographs in figure 9 for the NACA 1S-(70)(03)-(70)(03) at 5.5° angle of attack.

At a Mach number of 0.50 (fig. 9(a)) separated flow extended from the leading edge rearward and contributed toward an increased drag and reduced normal force. These conditions could have been predicted from low-speed considerations. When the Mach number was increased to 0.70, only two changes were noted. An increased expansion occurred around the leading edge (see dark area immediately above leading edge) and disturbances were observed in the main flow above the model, approximately 0.3 chord behind the leading edge. The increase in Mach number to 0.72 resulted in a further increase in the expansion region, a slight decrease in extent of separated flow above the surface, and a consolidation of the shocks. These changes were slightly intensified when the Mach number was increased to 0.75. The flow so far described (including $M = 0.75$) was in accord with that previously observed on subsonic airfoils. (For example, see reference 5.)

The increase in Mach number from 0.75 to 0.77 produced a change in the type of flow at the leading edge to one that had not previously been observed at subsonic speeds. At this higher Mach number (fig. 9(c)) oblique shocks were observed to extend outward into the flow from the vicinity of the leading edge and the separated flow over the forward part of the model had been eliminated. The main compression shock generally associated with airfoils at high subsonic speeds occurred near the 0.5-chord station. With further increase in Mach number to 0.80, the primary effects to be seen are the normally expected rearward movement of the main shock on the upper surface and the formation of shock on the lower surface. That this behavior of the flow is not peculiar to the condition

given in figure 9 is shown by figures 10 and 11. In figure 10 the unusual flow is observed at the leading edge of each of the supersonic airfoils at an angle of attack of 4° and a Mach number of 0.83. Figure 11 shows that for the NACA 1S-(30)(03)-(30)(03) airfoil the phenomenon occurred at an angle of attack of 2° as well as at 4°, and the field of influence decreased as the angle decreased until at 0° no unusual flow was observed. The sequences of flow photographs obtained at an angle of attack of 4° for each of the airfoils (not presented herein) indicated that the Mach number at which the flow phenomenon first occurred M_x decreased as the included angle of the leading edge θ increased, as shown in the following table:

NACA airfoil	θ (deg)	$M_x \pm 0.01$
1S-(70)(03)-(70)(03)	5.0	0.76
2S-(70)(03)-(70)(03)	9.8	.76
1S-(30)(03)-(30)(03)	11.4	.73
2S-(50)(03)-(50)(03)	13.8	.73
2S-(30)(03)-(30)(03)	23.3	.70

The leading-edge flow phenomenon through the elimination of the extensively separated flow over the forward part of the airfoil, would lead to an increase in normal force and a decrease in drag. At the same time, several factors exist which contribute to an increase in drag. These factors are the energy losses through the oblique shocks, the increased losses through the main shock having a greater intensity, and the losses because of separation from the surface in the vicinity of the main shock. The summation of all these effects would lead to an increase in normal force and an unpredictable effect on drag. An examination of figure 3 will show that the rate of change of section normal-force coefficient with Mach number is greater above the Mach number at which the oblique shock first appeared at the leading edge of the airfoil. Figure 6 (or fig. 7(b)), however, showed that the Mach number increment between the value at which the flow change occurred and the value at which the drag coefficient began to increase very rapidly varied from 0 for the NACA 1S-(70)(03)-(70)(03) (fig. 6(g)) to 0.07 for the NACA 2S-(30)(03)-(30)(03) (fig. 6(c)). In addition, figure 6 also showed that for the NACA 2S-(70)(03)-(70)(03) and NACA 1S(30)(03)-(30)(03) airfoils (figs. 6(e) and 6(f)) a marked decrease in drag coefficient was obtained after the flow change occurred. The possibility that this new type of flow at the leading edge could have an appreciable effect on the maximum lift of airfoils at high subsonic Mach numbers indicates the desirability of extending the original investigation on supersonic airfoils to obtain data at higher angles of attack.

Additional information on the observed flow phenomenon was obtained by measuring the static pressures at the tunnel wall near the leading edge of the model. Data obtained thereby, as well as the pressures measured along the surface of the model, were transcribed into local Mach numbers and are presented in figure 12, together with the corresponding schlieren photographs of the flow. The local Mach numbers of figure 12 were based on the total pressure in the undisturbed stream and are therefore high for regions behind shocks and within separated flows.

At a stream Mach number of 0.80 for the NACA 1S-(70)(03)-(70)(03) at 4° angle of attack (fig. 12(a)) the flow-field measurements showed that the local Mach numbers were supersonic in a plane normal to the leading edge of the airfoil and for a distance of at least 0.2 chords above it. This position falls within the dark area or region of expansion above the leading edge of the airfoil in the schlieren photograph. Both schlieren photograph and flow-field measurements showed that further increases in velocity or expansions occurred rearward of the leading edge. An expansion at supersonic speeds is accompanied without energy losses by a change in direction of flow or a Prandtl-Meyer turn (reference 6). The change in flow direction is such that the air is directed toward the surface of the airfoil. Obviously, in this case (and in figs. 12(b) and 10), the flow is directed into the surface of the airfoil, which necessitates an oblique shock to turn the flow somewhat in the other direction so that the air can flow along the model surface, and the extensive separated-flow condition is thus eliminated. The flow behind the oblique shock is supersonic and the shock generally associated with airfoils at high subsonic Mach numbers is encountered rearward on the airfoil.

The foremost and weak oblique shock seen in the schlieren photograph of figure 12(a) appeared from an analysis of schlieren photographs and flow-field measurements to be an envelope of disturbances originating from the leading edge. The conditions under which the weak shock formed appeared to be the existence of supersonic velocities in the vicinity of the leading edge and a highly localized separated region originating at the leading edge and extending rearward only a few percent of the chord. The point at which the flow became reattached to the surface became the origin of the more intense oblique shock that turned the air so that it flowed along the surface. (See also figs. 9(e) and 9(f) and 10(b) and 10(c).)

The data presented in figure 12(b) for the NACA 1S-(30)(03)-(30)(03) airfoil at 4° were generally similar to those of figure 12(a) except that the velocities in the plane above and normal to the

leading edge were slightly less than sonic and, in place of the dual oblique shocks seen in figure 12(a), only one was apparent in figure 12(b). Figures 9, 10, and 12 could leave the impression that the single oblique shock as in figure 12(b) would occur only on those airfoils having an included angle greater than 10°. No such conclusion is justified, as could be shown by other schlieren photographs of the series.

Figure 12(c) and the previous discussion of figure 11 showed that no unusual flow change occurred at the leading edge of the NACA 1S-(30)(03)-(30)(03) at 0° angle of attack. At the 0.3-chord station, however, where an 8.2° change occurred in the slope of the airfoil surface, a flow condition existed at high Mach numbers (fig. 12(c)) that had some similarity to the flow phenomena previously described. The Prandtl-Meyer turn at the 0.3-chord station tended to exceed the 8.2° turn allowed by the surface, thereby necessitating an immediate compression as shown by both schlieren photographs and the airfoil surface pressure measurements. (See fig. 2(g).) The gradual compression that followed is probably a result of a progressively increasing boundary-layer thickness, as is shown in figure 12(a).

The present investigation also showed that the unusual flow phenomenon was not strictly limited to airfoils having sharp leading edges. The intensity of the oblique shock shown near the leading edge in figure 13 indicates that the magnitude of the Prandtl-Meyer turn diminished markedly when the leading-edge radius increased from 0 for the NACA 2S-(30)(03)-(30)(03) airfoil to 0.22 percent chord for the NACA 66-006 airfoil. The effect for the NACA 0006-63 airfoil having a 0.4-percent-chord radius is almost imperceptible.

CONCLUDING REMARKS

A two-dimensional investigation of supersonic airfoils indicated that at subsonic Mach numbers, although the drag characteristics were in general higher for these airfoils than for subsonic airfoils, the normal-force and pitching-moment characteristics of those supersonic profiles having their maximum thickness located at the 0.7-chord station would diminish the problems generally encountered in longitudinal control at high subsonic Mach numbers.

The investigation also revealed the occurrence of an unusual flow phenomenon at the leading edges of the supersonic profiles. This phenomenon, through elimination of the extensive separated-flow condition over the forward part of the airfoil, effected an increase

in normal force and produced changes ranging from no effect to a decrease in the drag coefficient. Further, it appears possible that the flow phenomenon could have an appreciable effect on the maximum lift coefficient of supersonic airfoils at high subsonic Mach numbers.

Langley Memorial Aeronautical Laboratory,
National Advisory Committee for Aeronautics
Langley Field, Va., August 12, 1946

REFERENCES

1. Stack, John, and von Doenhoff, Albert E.: Tests of 16 Related Airfoils at High Speeds. NACA Rep. No. 492, 1934.

2. Briggs, L. J., and Dryden, H. L.: Aerodynamic Characteristics of Twenty-Four Airfoils at High Speeds. NACA Rep. No. 319, 1929.

3. Abbott, Ira H., von Doenhoff, Albert E., and Stivers, Louis S., Jr.: Summary of Airfoil Data. NACA ACR No. L5C05, 1945.

4. Allen, H. Julian, and Vincenti, Walter G.: Wall Interference in a Two-Dimensional-Flow Wind Tunnel with Consideration of the Effect of Compressibility. NACA ARR No. 4K03, 1944.

5. Stack, John: Compressible Flows in Aeronautics. Jour. Aero. Sci., vol. 12, no. 2, April 1945, pp. 127-143.

6. Taylor, G. I., and Maccoll, J. W.: The Mechanics of Compressible Fluids. Two-Dimensional Flow at Supersonic Speeds. Vol. III of Aerodynamic Theory, div. H, ch. IV, sec. 4 and 5, W. F. Durand, ed., Julius Springer (Berlin), 1935, pp 242-246.

TABLE I.- BASIC SECTION ORDINATES FOR SYMMETRICAL CIRCULAR-ARC AIRFOILS

[Stations and ordinates are in percent chord]

Station	Ordinate		
	2S-(30)(03)-(30)(03)	2S-(50)(03)-(50)(03)	2S-(70)(03)-(70)(03)
0	0	0	0
5	.92	.57	.40
10	1.67	1.08	.79
15	2.25	1.53	1.15
20	2.67	1.92	1.47
25	2.92	2.25	1.76
30	3.00	2.52	2.02
35	2.98	2.73	2.25
40	2.94	2.88	2.45
45	2.86	2.97	2.61
50	2.75	3.00	2.75
55	2.61	2.97	2.86
60	2.45	2.88	2.94
65	2.25	2.73	2.98
70	2.02	2.52	3.00
75	1.76	2.25	2.92
80	1.47	1.92	2.67
85	1.15	1.53	2.25
90	0.79	1.08	1.67
95	0.40	0.57	0.92
100	0	0	0
L.E. radius: 0			

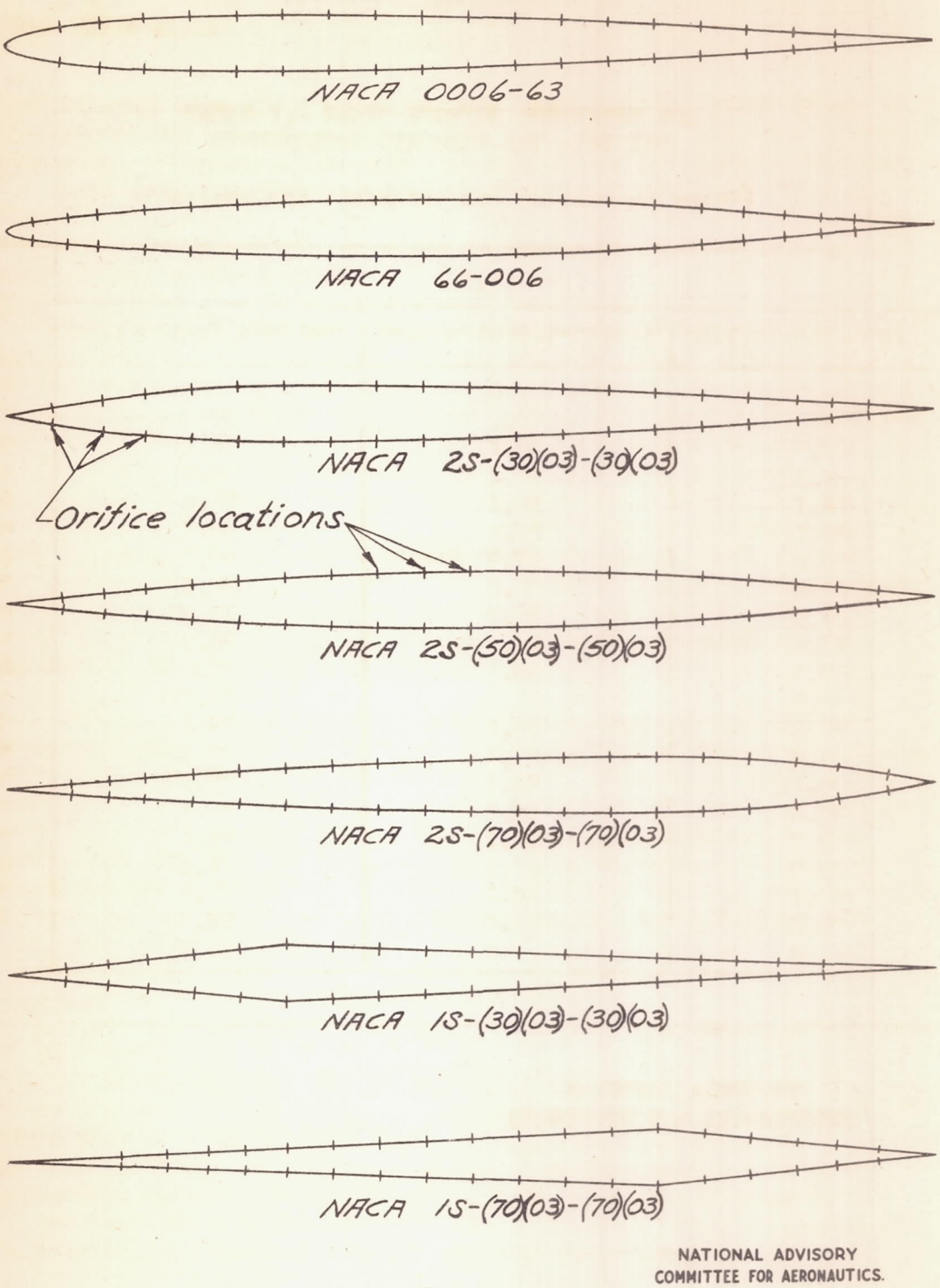

Figure 1.- Airfoil profiles and static-pressure-orifice locations.

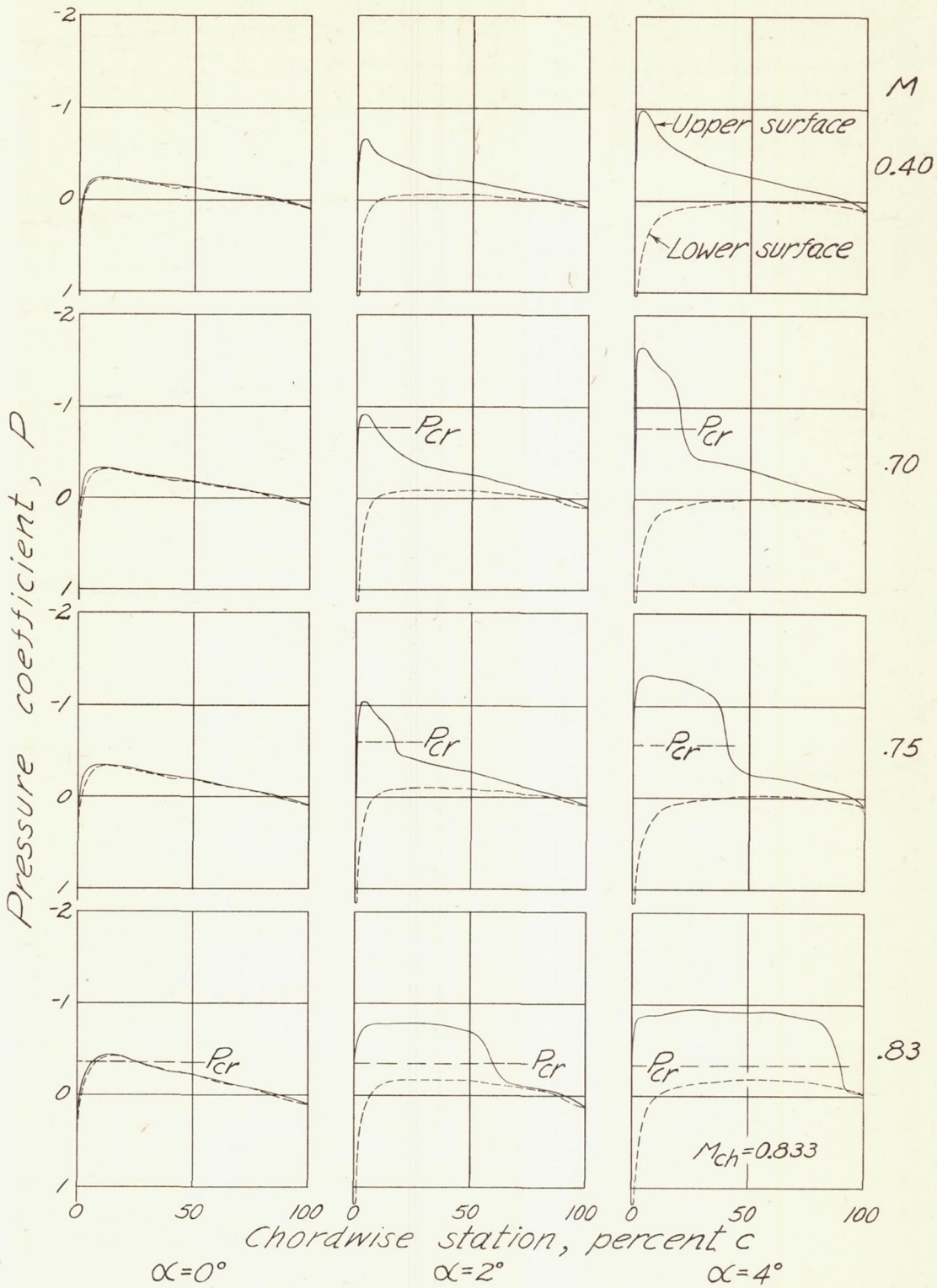

(a) NACA 0006-63 airfoil.

NATIONAL ADVISORY COMMITTEE FOR AERONAUTICS

Figure 2. - Representative pressure distributions.

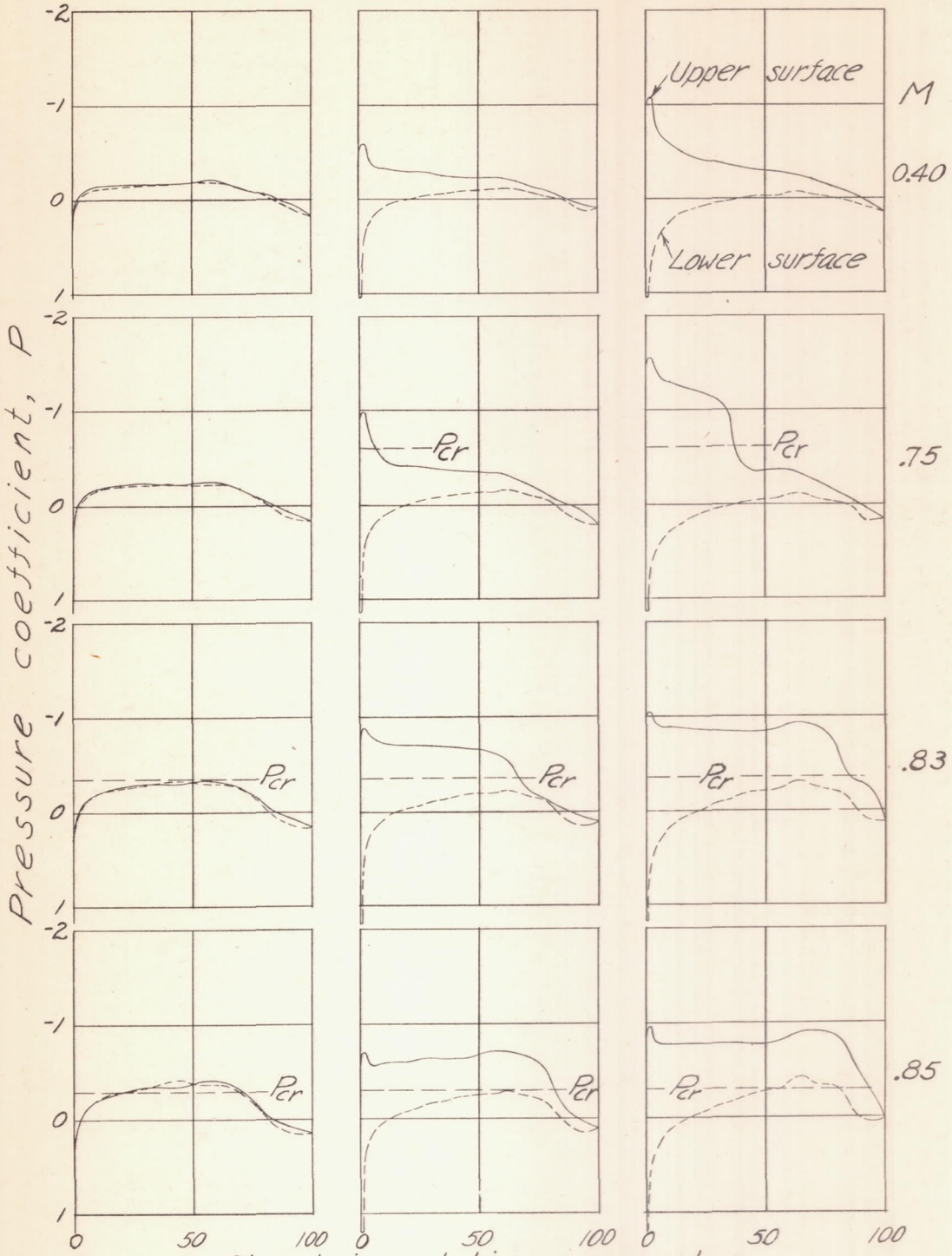

(b) NACA 66-006 airfoil.

NATIONAL ADVISORY COMMITTEE FOR AERONAUTICS

Figure 2.- Continued.

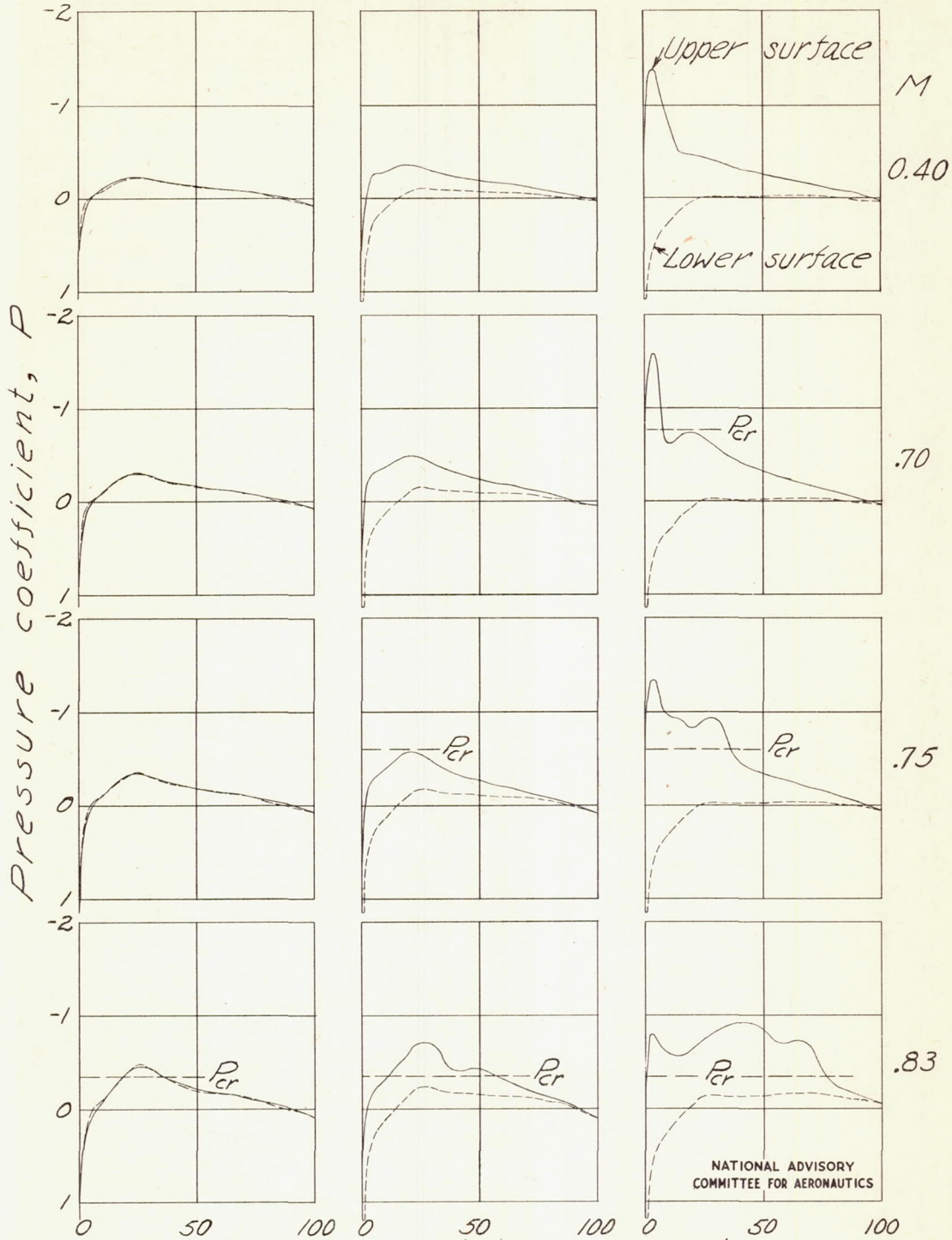

$\alpha = 0°$ $\alpha = 2°$ $\alpha = 4°$

(c) NACA 2S-(30)(03)-(30)(03) airfoil.

Figure 2.- Continued.

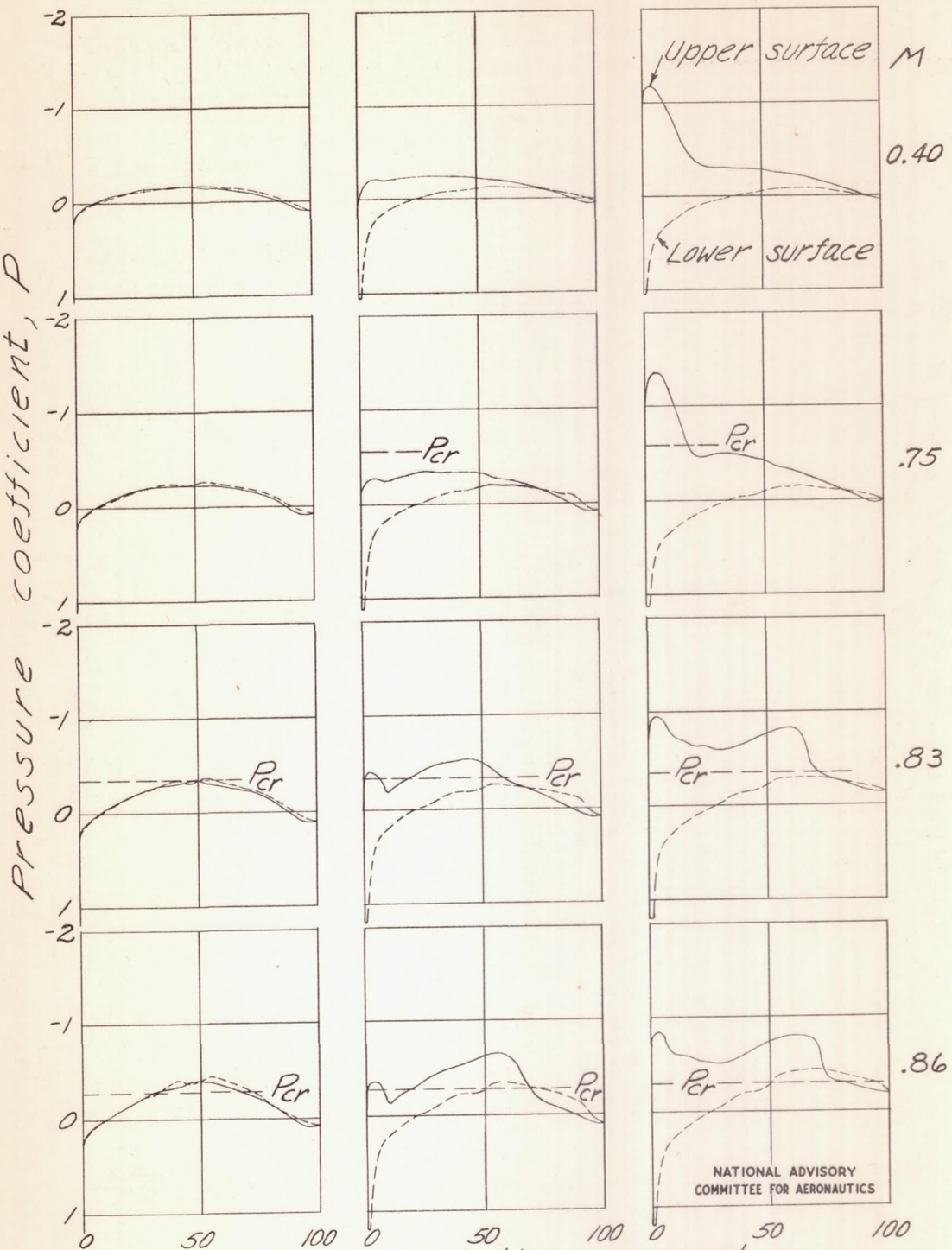

(d) NACA 2S-(50)(03)-(50)(03) airfoil.

Figure 2.- Continued.

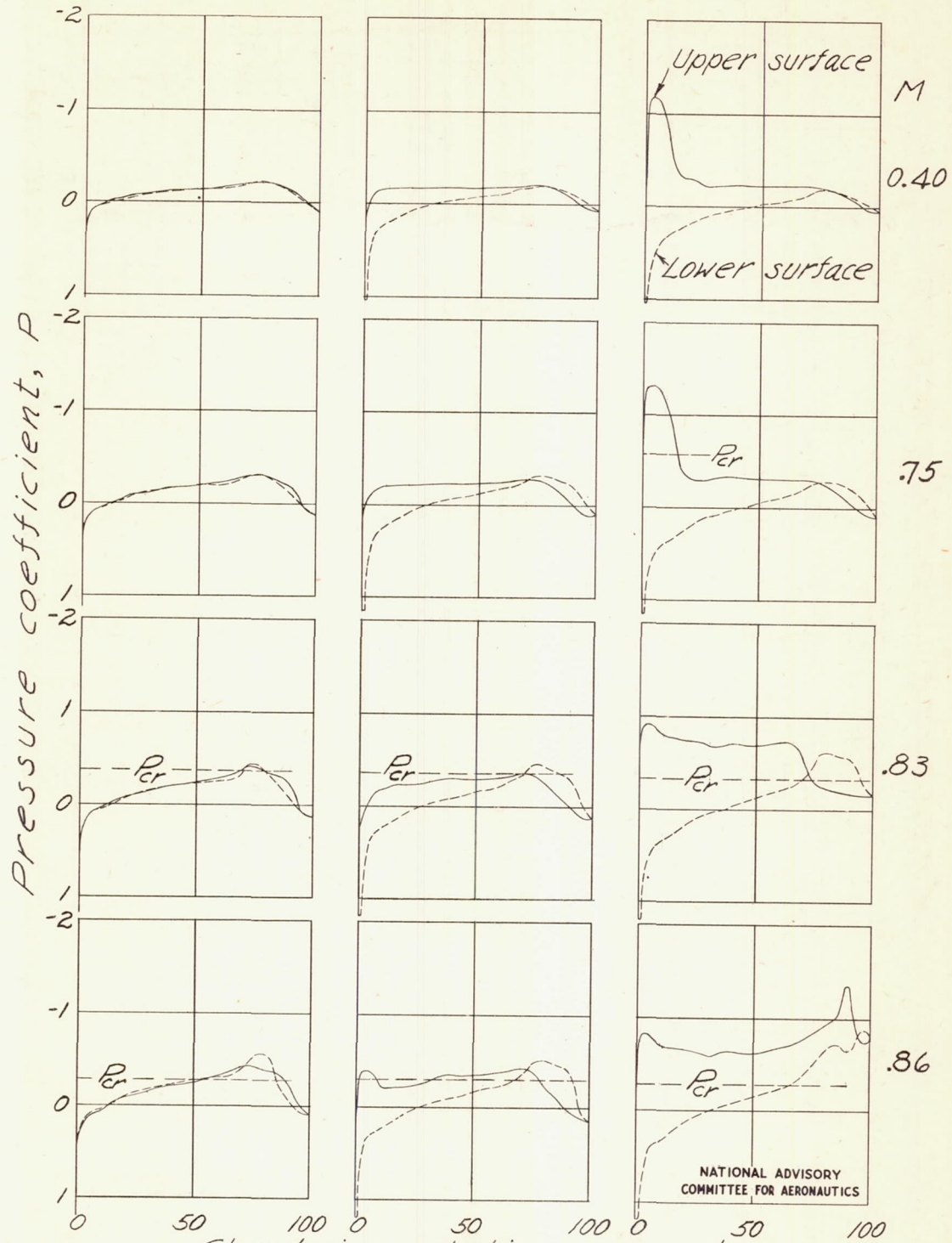

(e) NACA 2S-(70)(03)-(70)(03) airfoil.

Figure 2.- Continued.

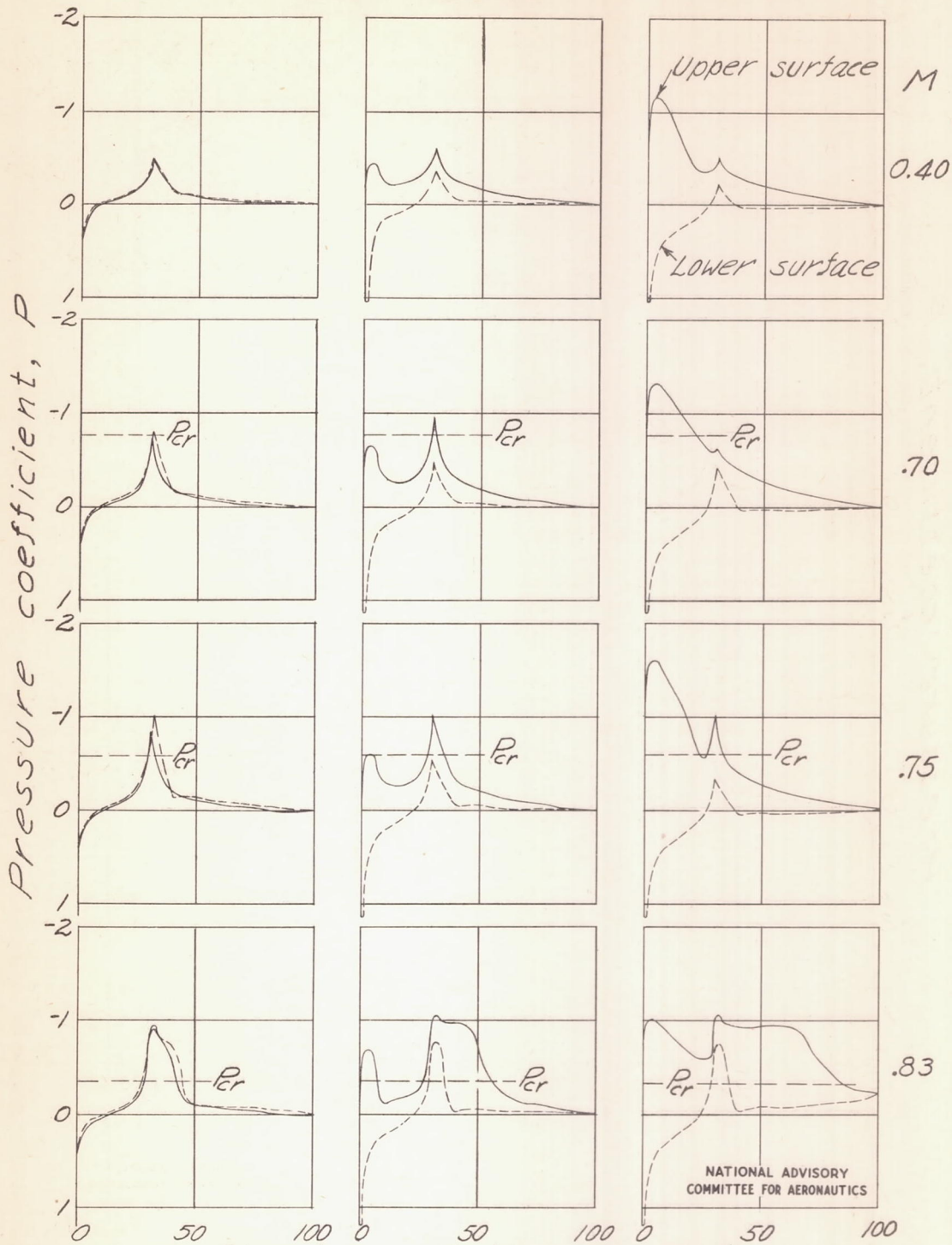

(f) NACA 1S-(30)(03)-(30)(03) airfoil.

Figure 2.- Continued.

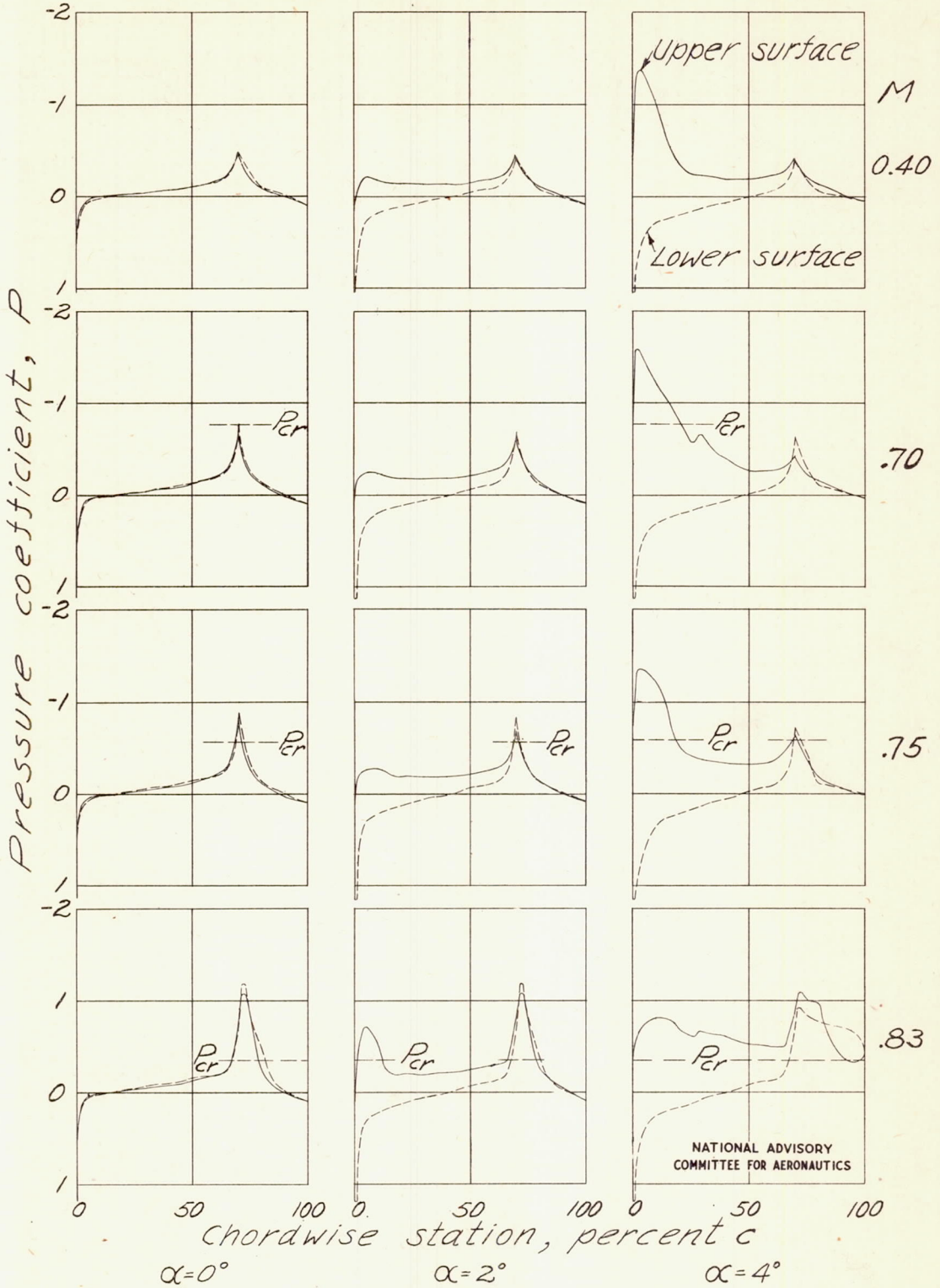

(g) NACA 1S-(70)(03)-(70)(03) airfoil.

Figure 2.- Concluded.

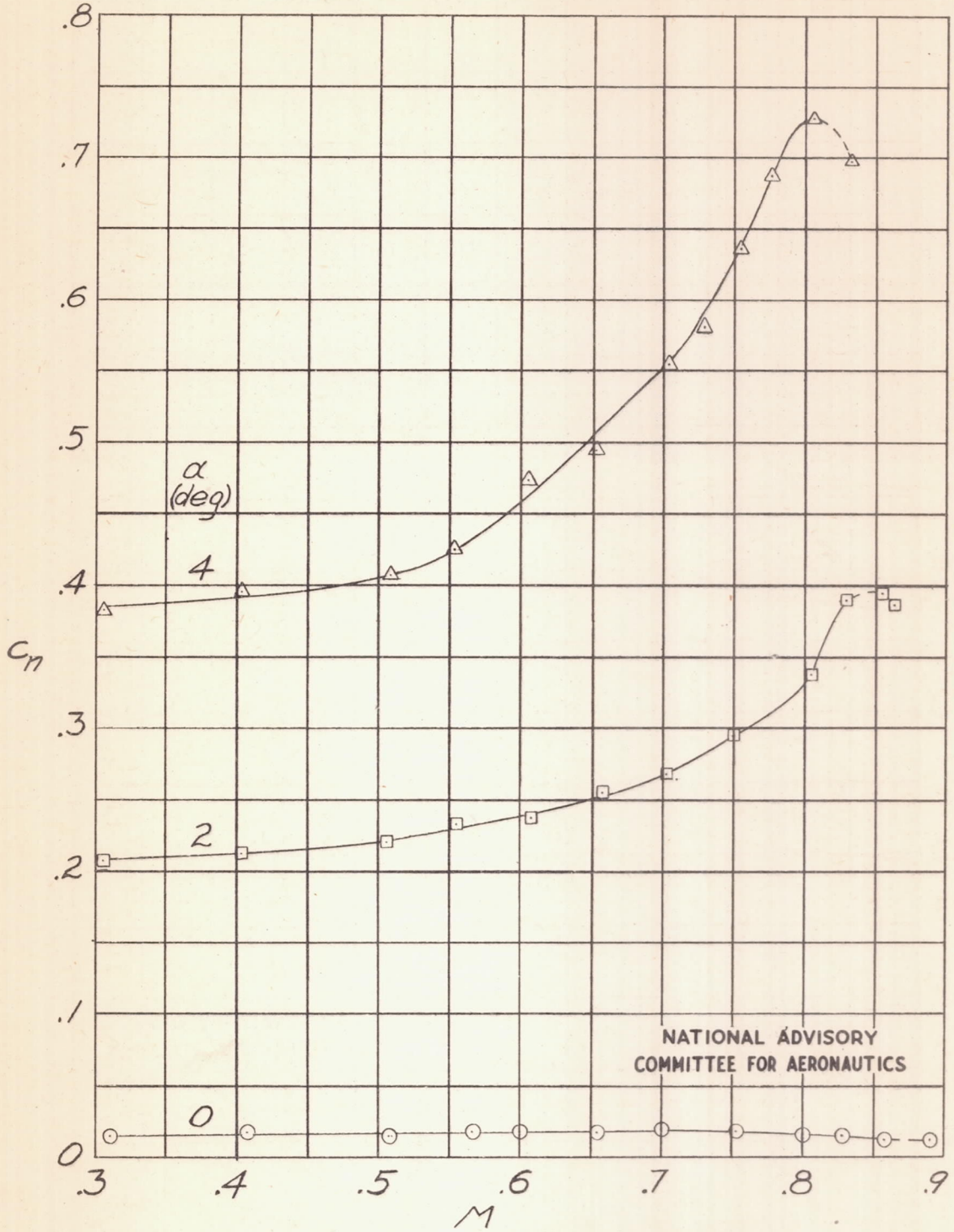

(a) NACA 0006-63 airfoil.

Figure 3.— Variation of section normal-force coefficient c_n with Mach number M.

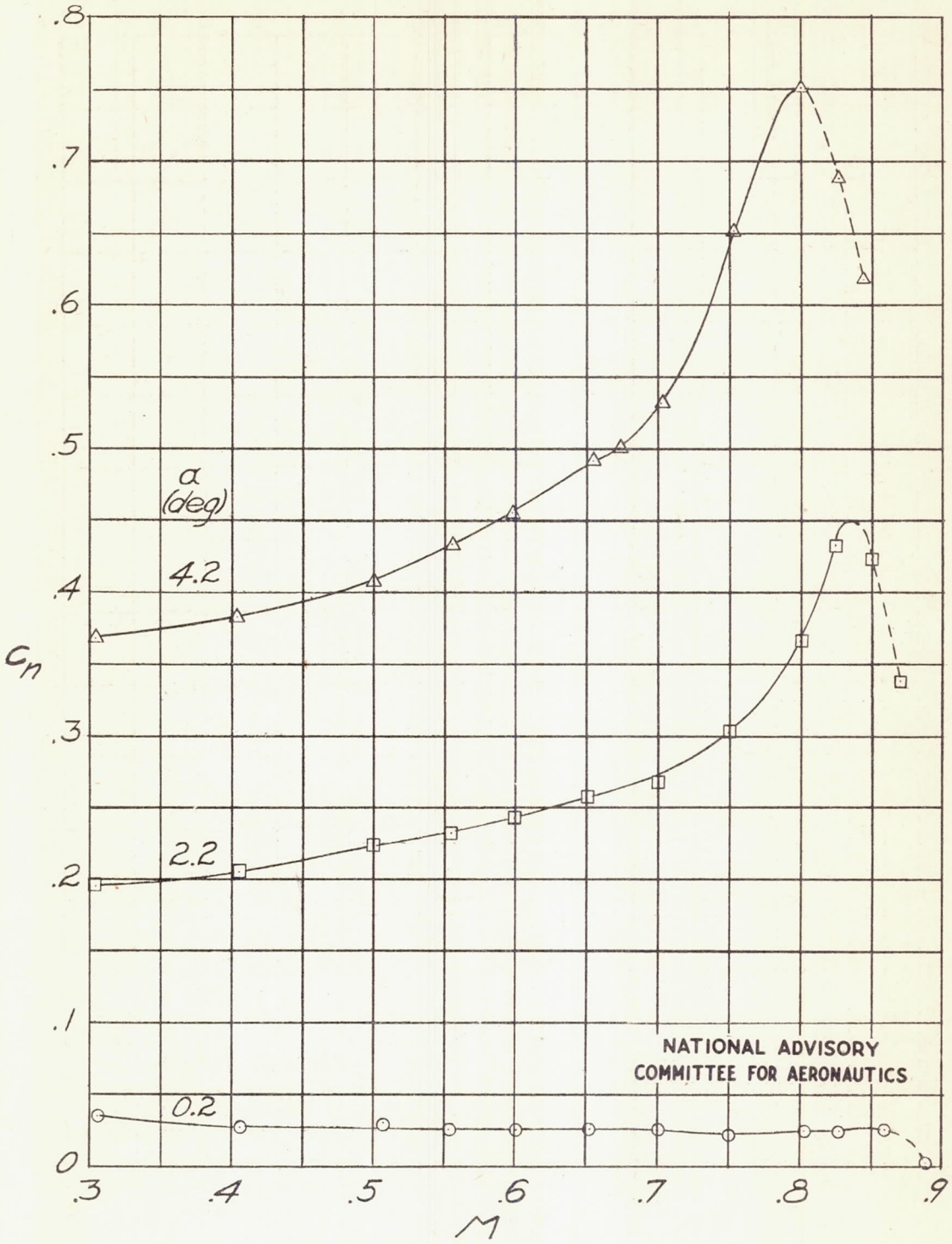

(b) NACA 66-006 airfoil.

Figure 3.—Continued.

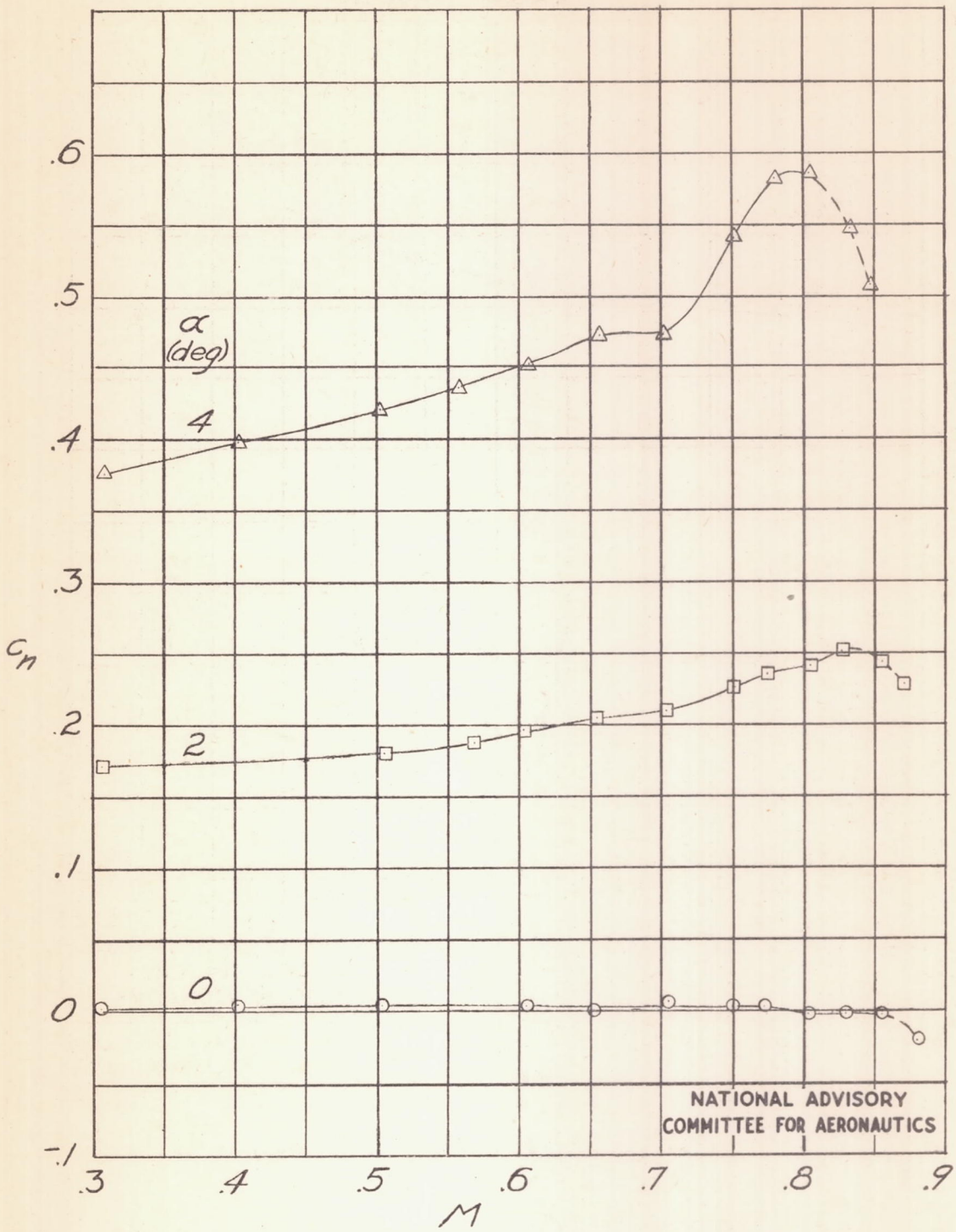

(c) NACA 2S-(30)(03)-(30)(03) airfoil.

Figure 3.- Continued.

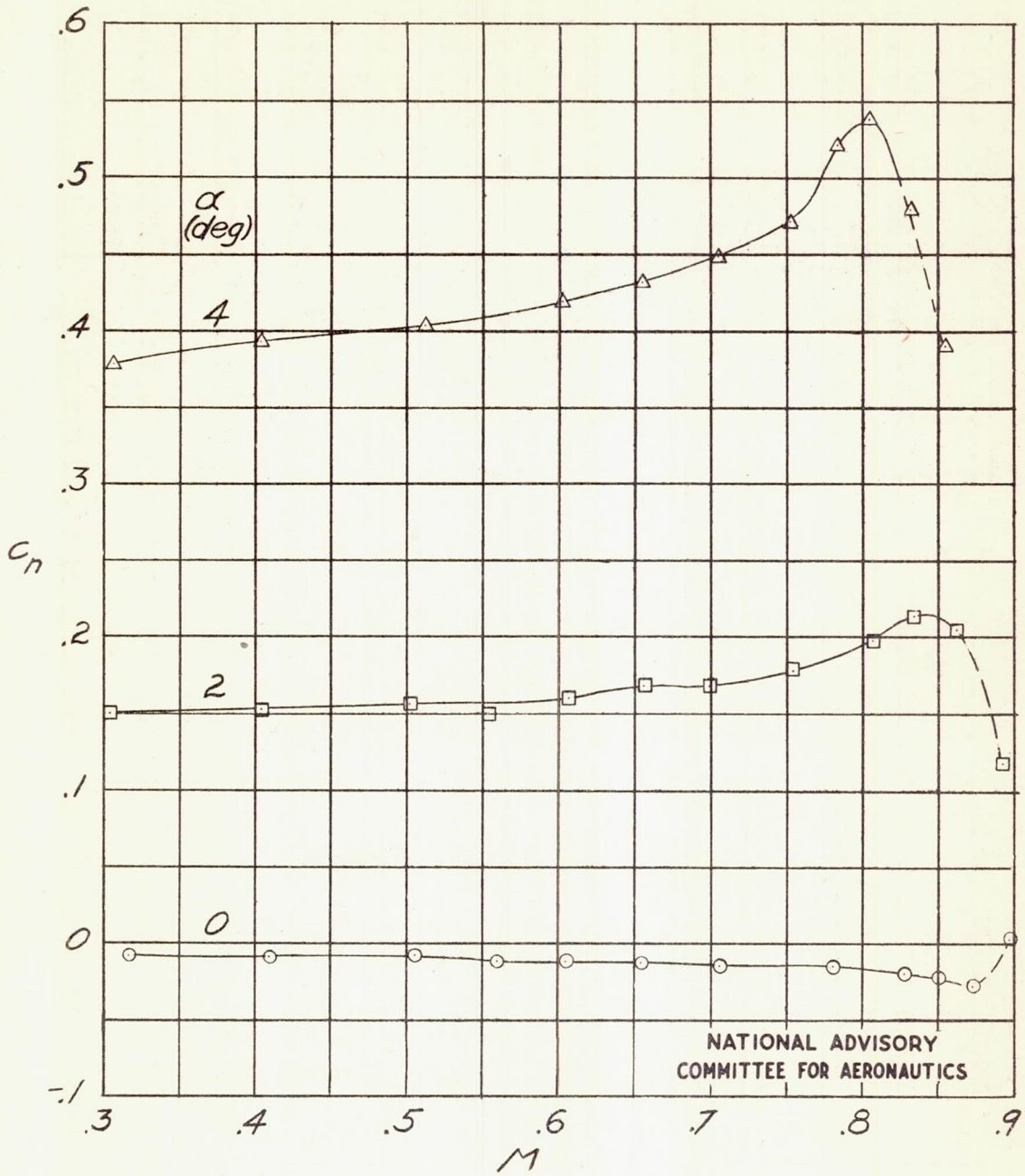

(d) NACA 2S-(50)(03)-(50)(03) airfoil.

Figure 3.- Continued.

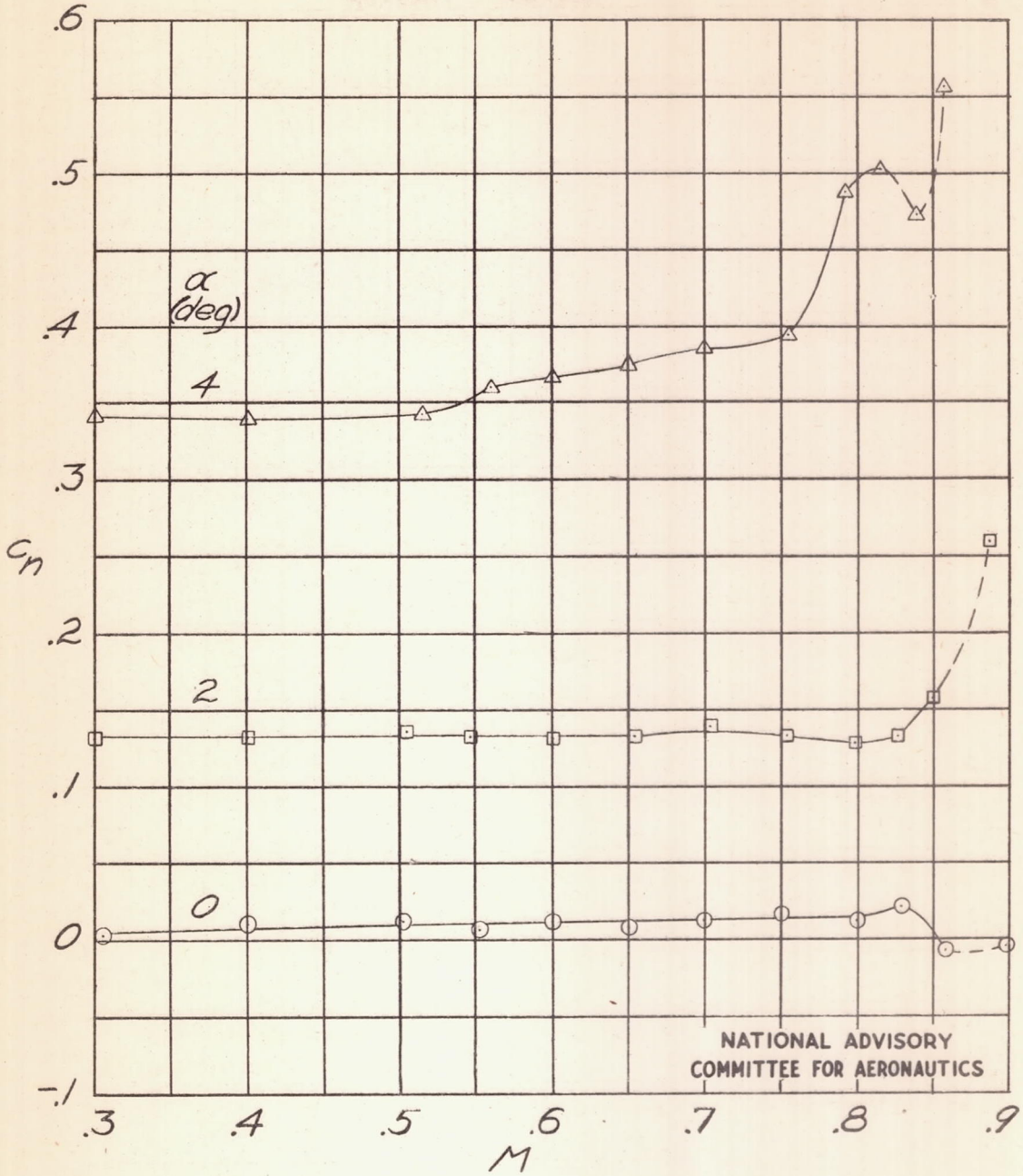

(e) NACA 2S-(70)(03)-(70)(03) airfoil.

Figure 3.- Continued.

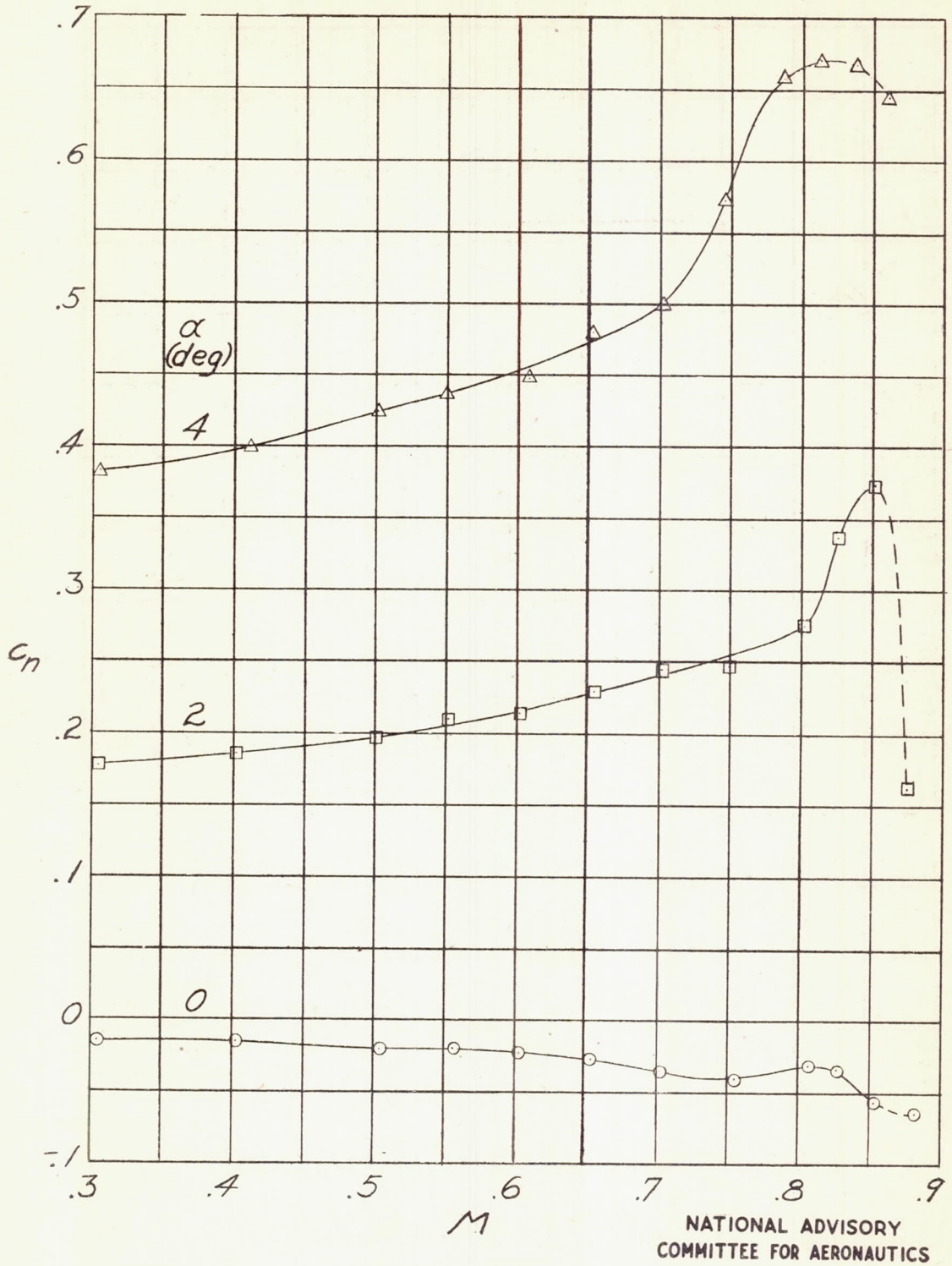

(f) NACA 1S-(30)(03)-(30)(03) airfoil.

Figure 3.- Continued.

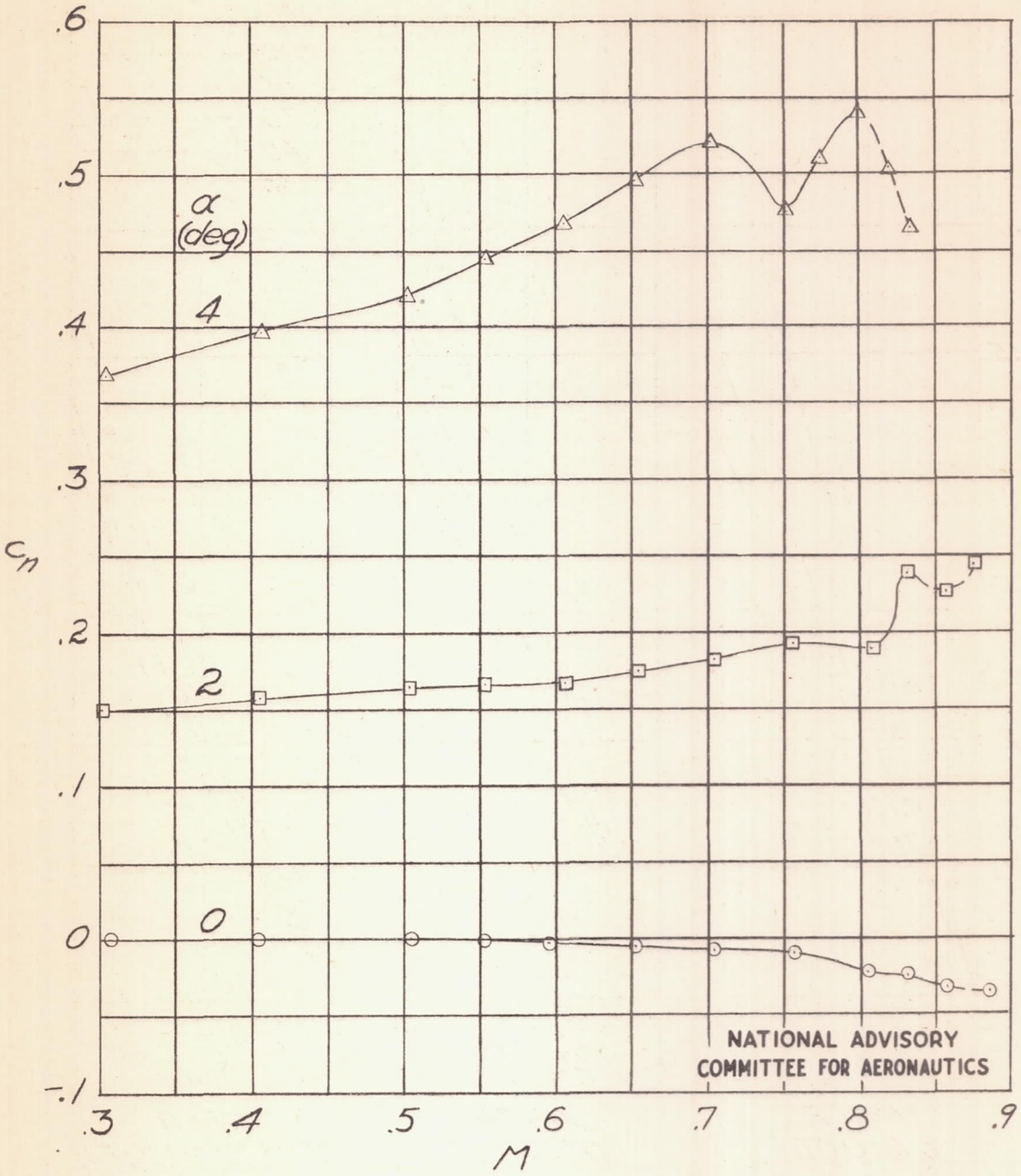

(g) NACA 1S-(70)(03)-(70)(03) airfoil.

Figure 3.- Concluded.

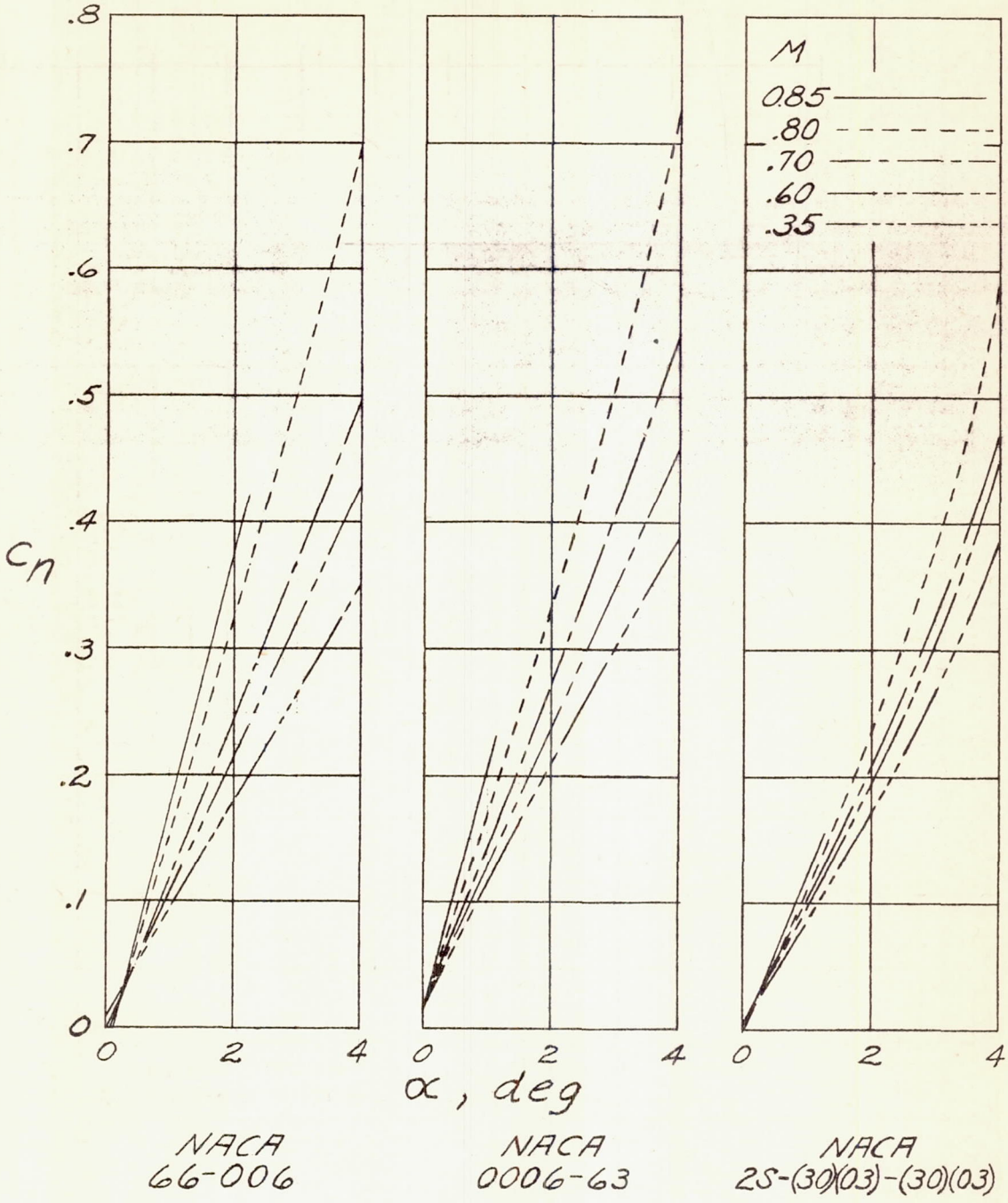

(a) Effect of Mach number.

Figure 4.-Variation of section normal-force coefficient c_n with angle of attack α.

NATIONAL ADVISORY COMMITTEE FOR AERONAUTICS

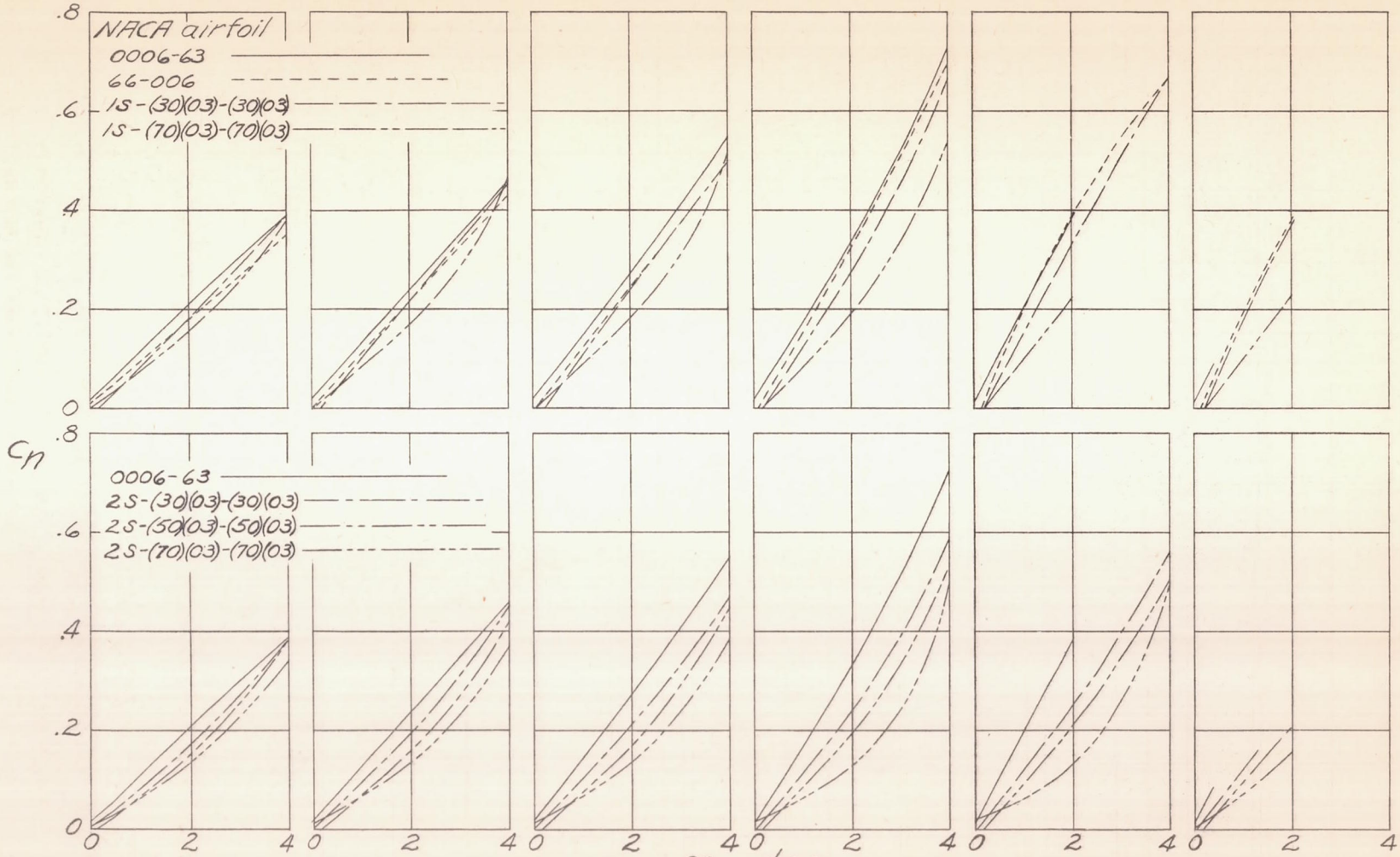

(b) Effect of airfoil shape.

Figure 4.-Concluded.

NATIONAL ADVISORY COMMITTEE FOR AERONAUTICS

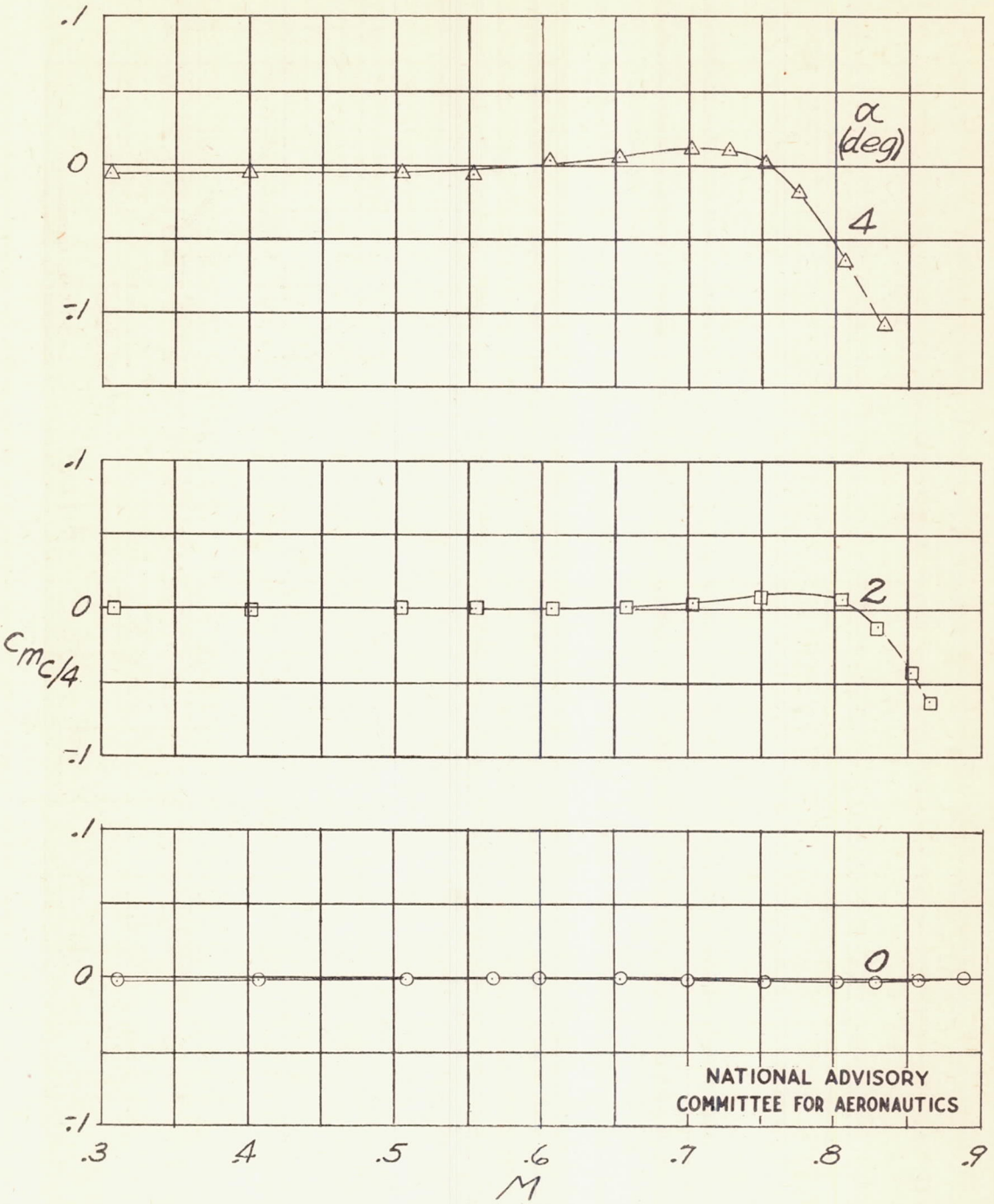

(a) NACA 0006-63 airfoil.

Figure 5.- Variation of section pitching-moment coefficient $c_{m_{c/4}}$ with Mach number M.

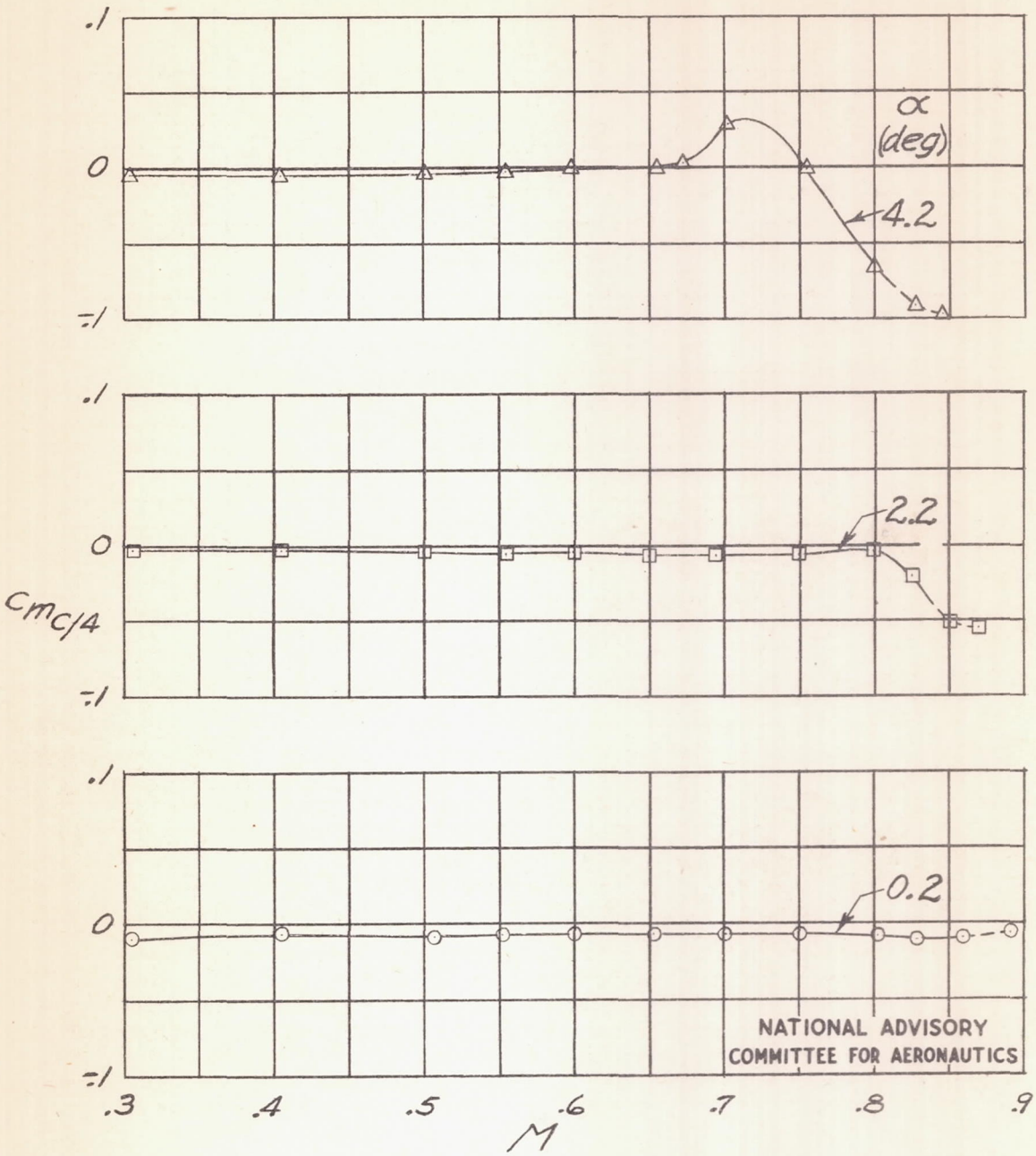

(b) NACA 66-006 airfoil.

Figure 5.- Continued.

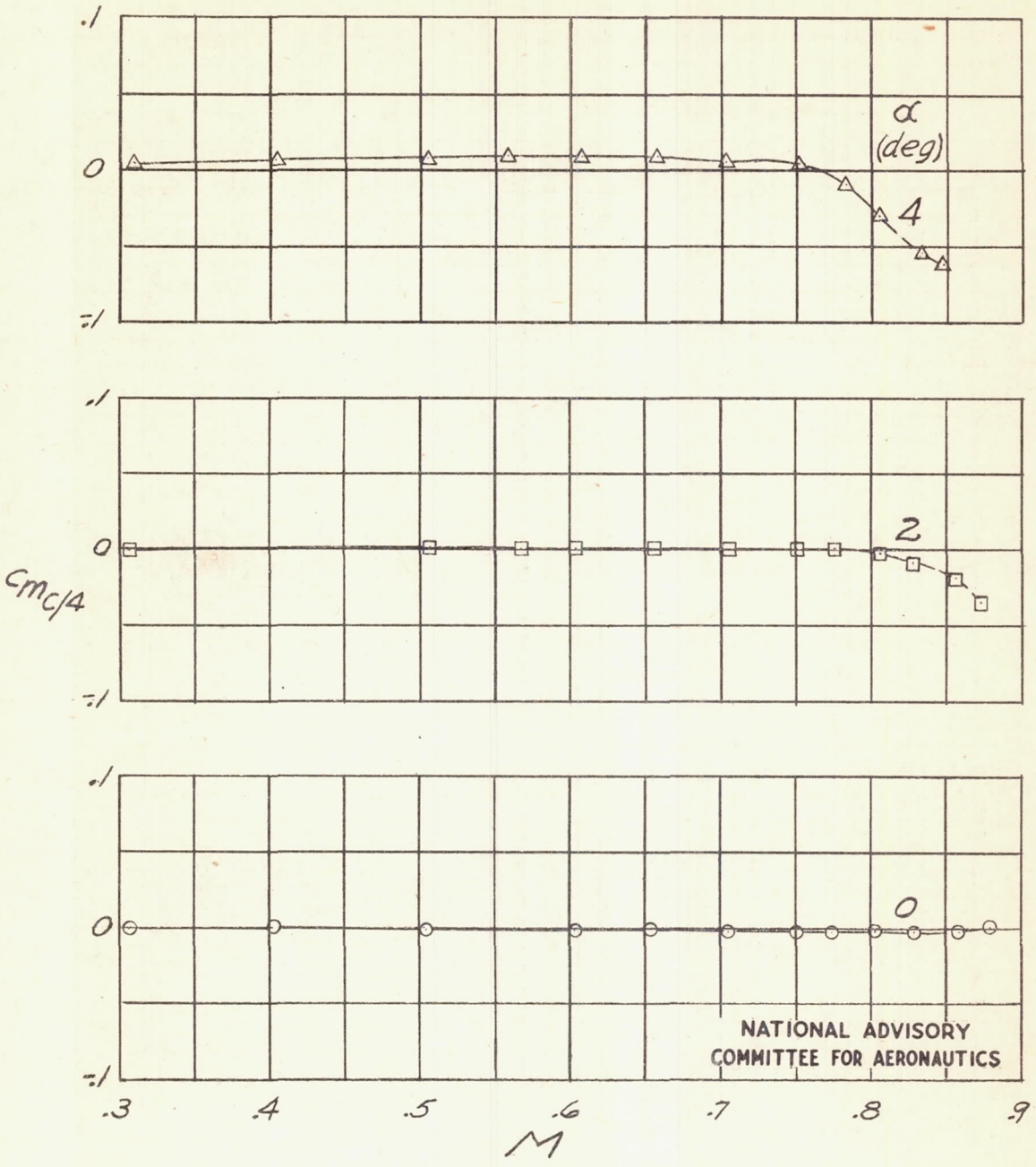

(c) NACA 25-(30)(03)-(30)(03) airfoil.

Figure 5.- Continued.

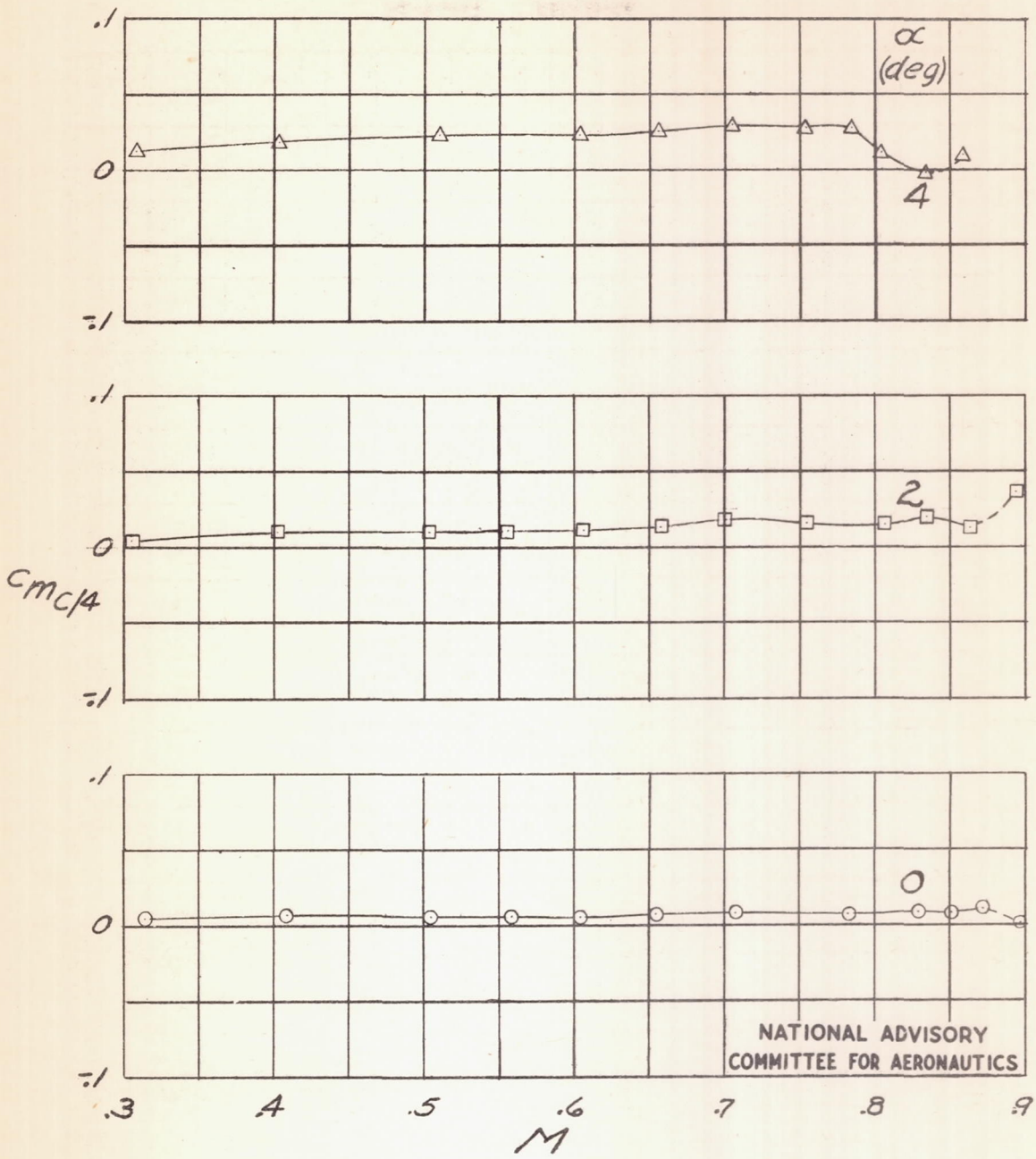

(d) NACA 25-(50)(03)-(50)(03) airfoil.

Figure 5.- Continued.

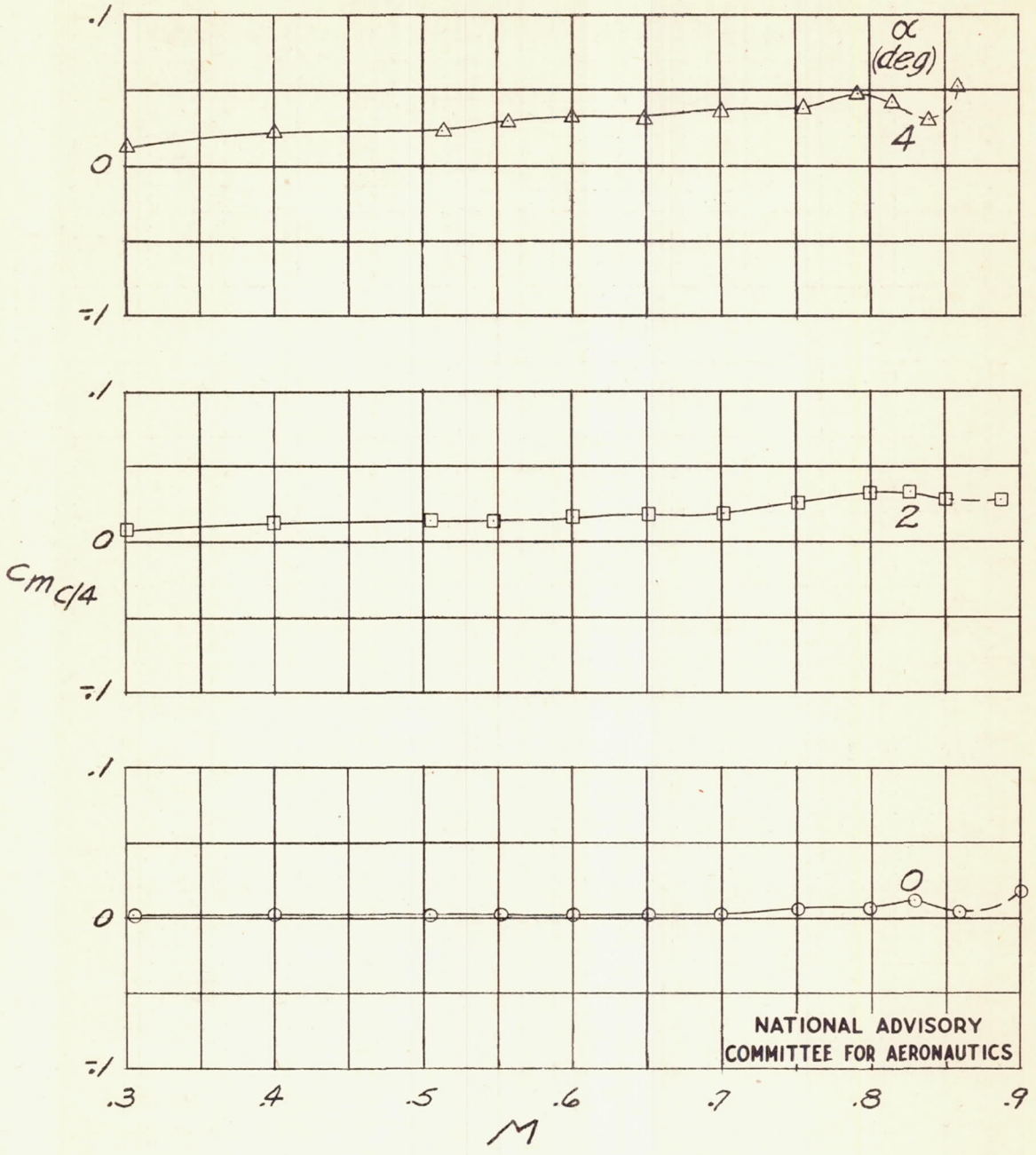

(e) NACA 2S-(70)(03)-(70)(03) airfoil.

Figure 5.- Continued.

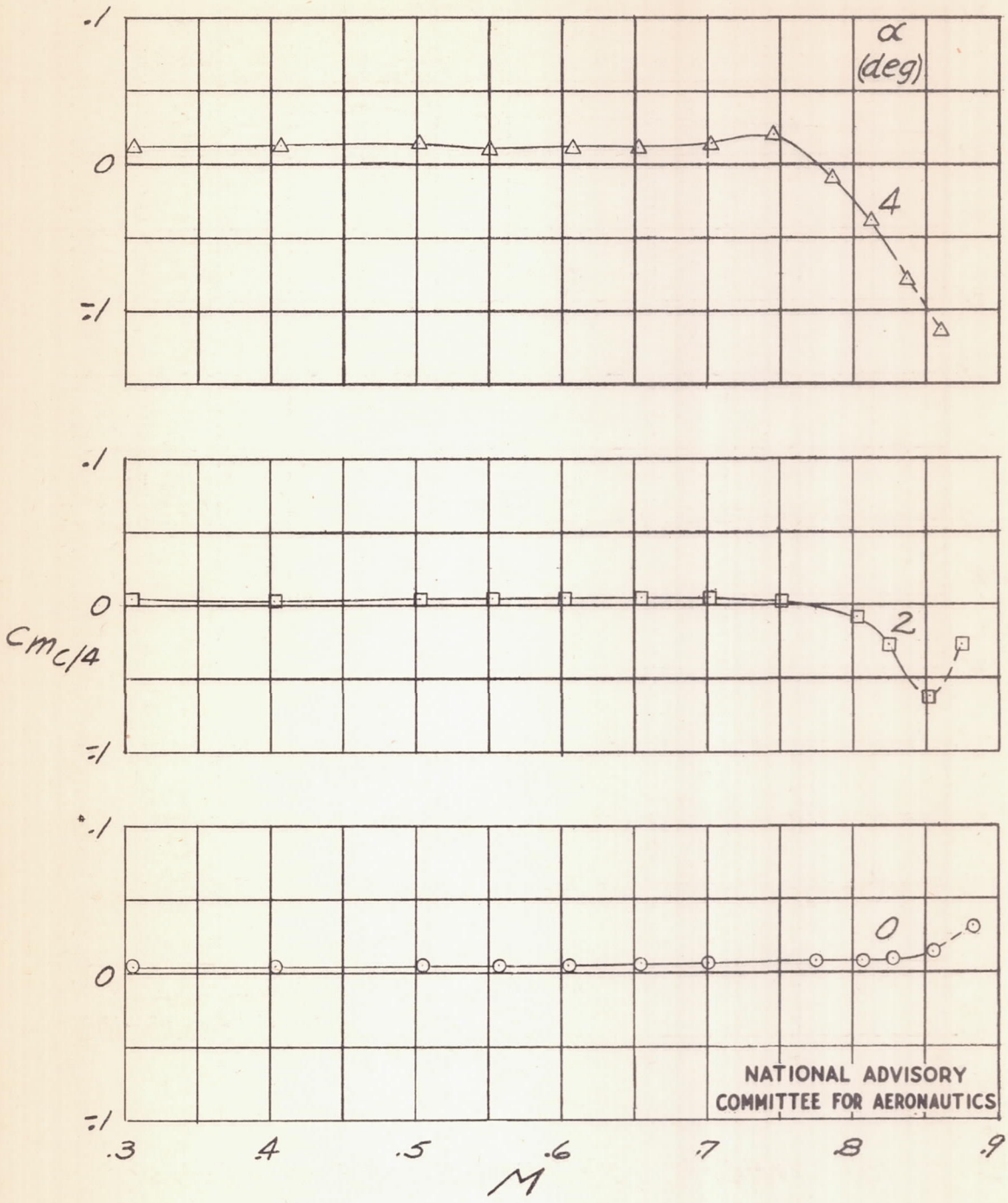

(f) NACA 1S-(30)(03)-(30)(03) airfoil.

Figure 5.-Continued.

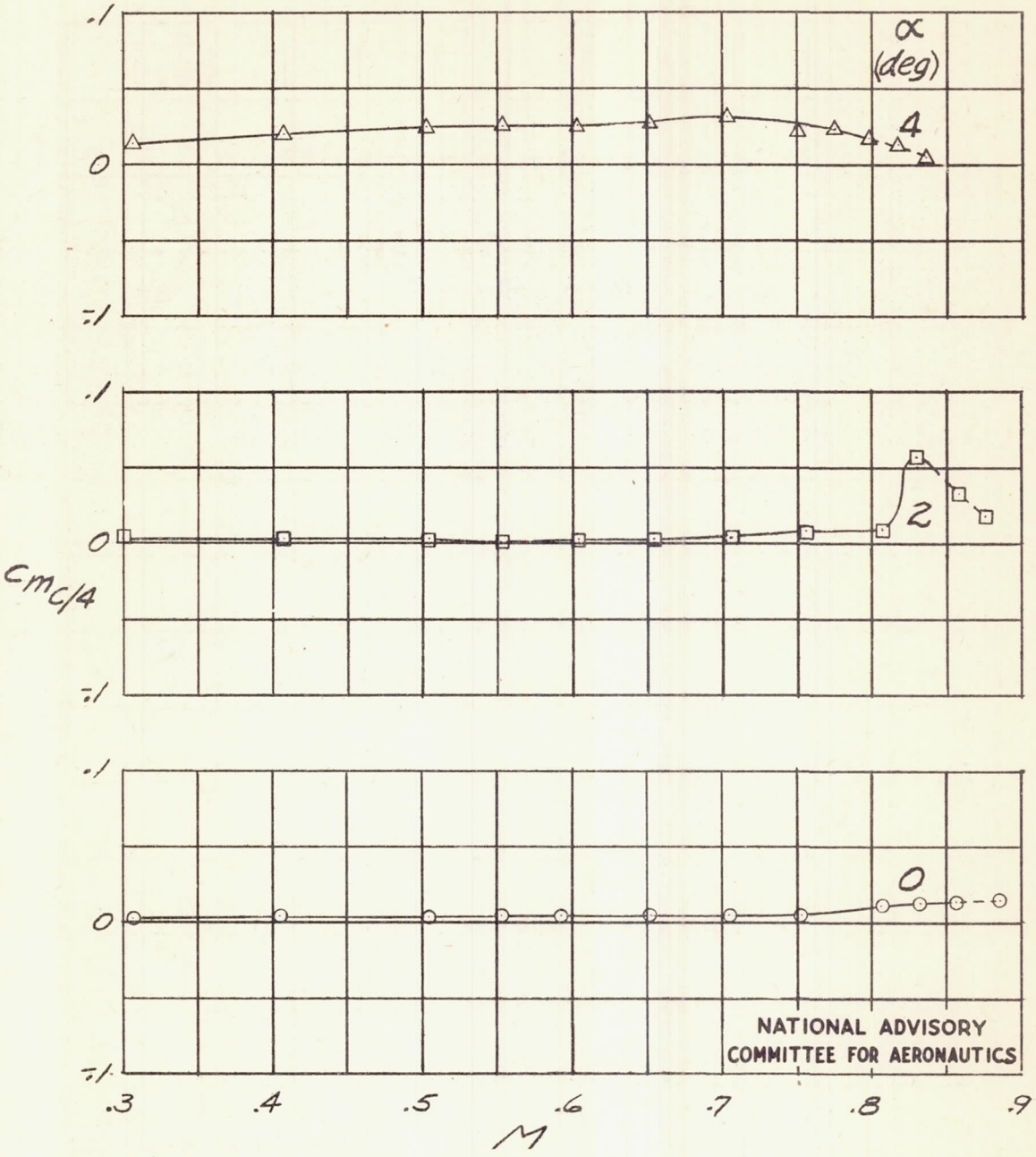

(g) NACA 1S-(70)(03)-(70)(03) airfoil.

Figure 5.- Concluded.

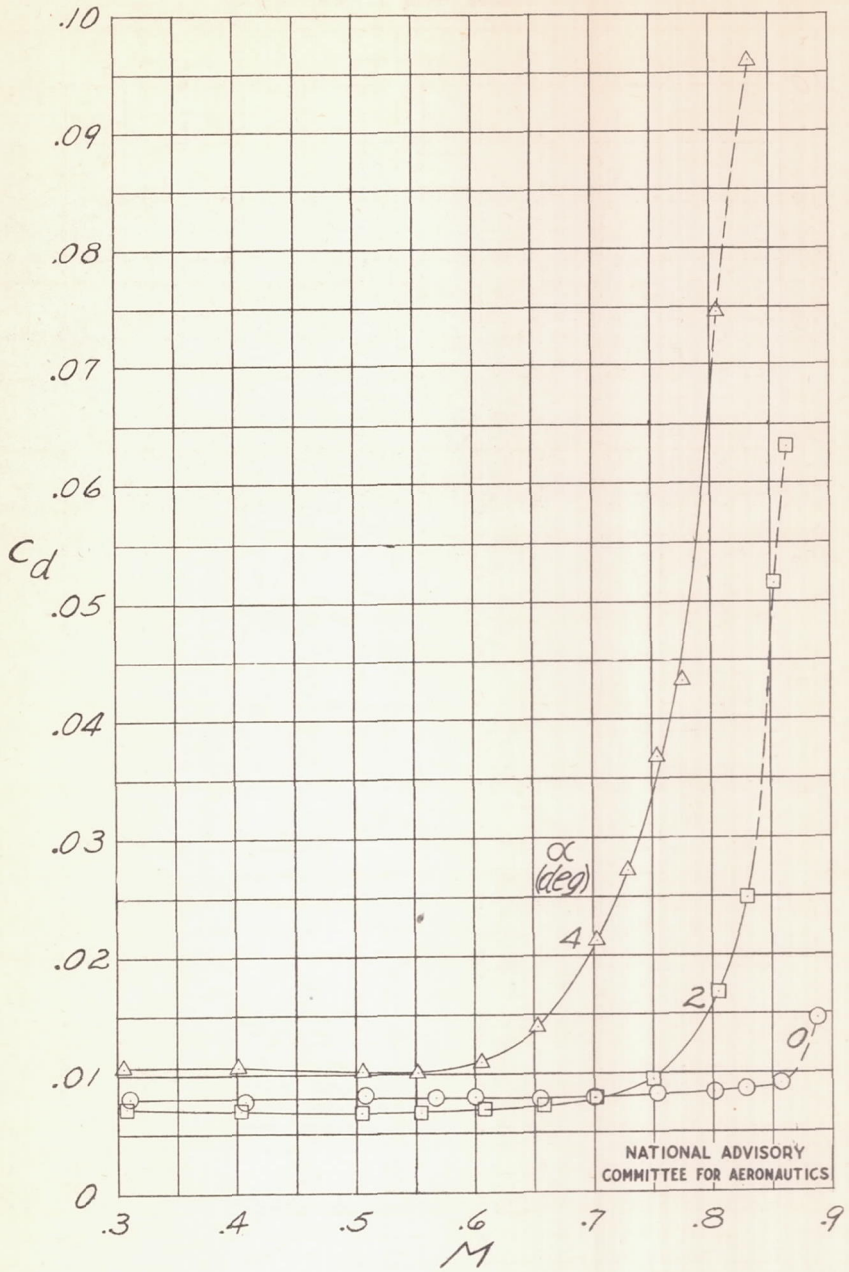

(a) NACA 0006-63 airfoil.

Figure 6.- Variation of section drag coefficient c_d with Mach number M.

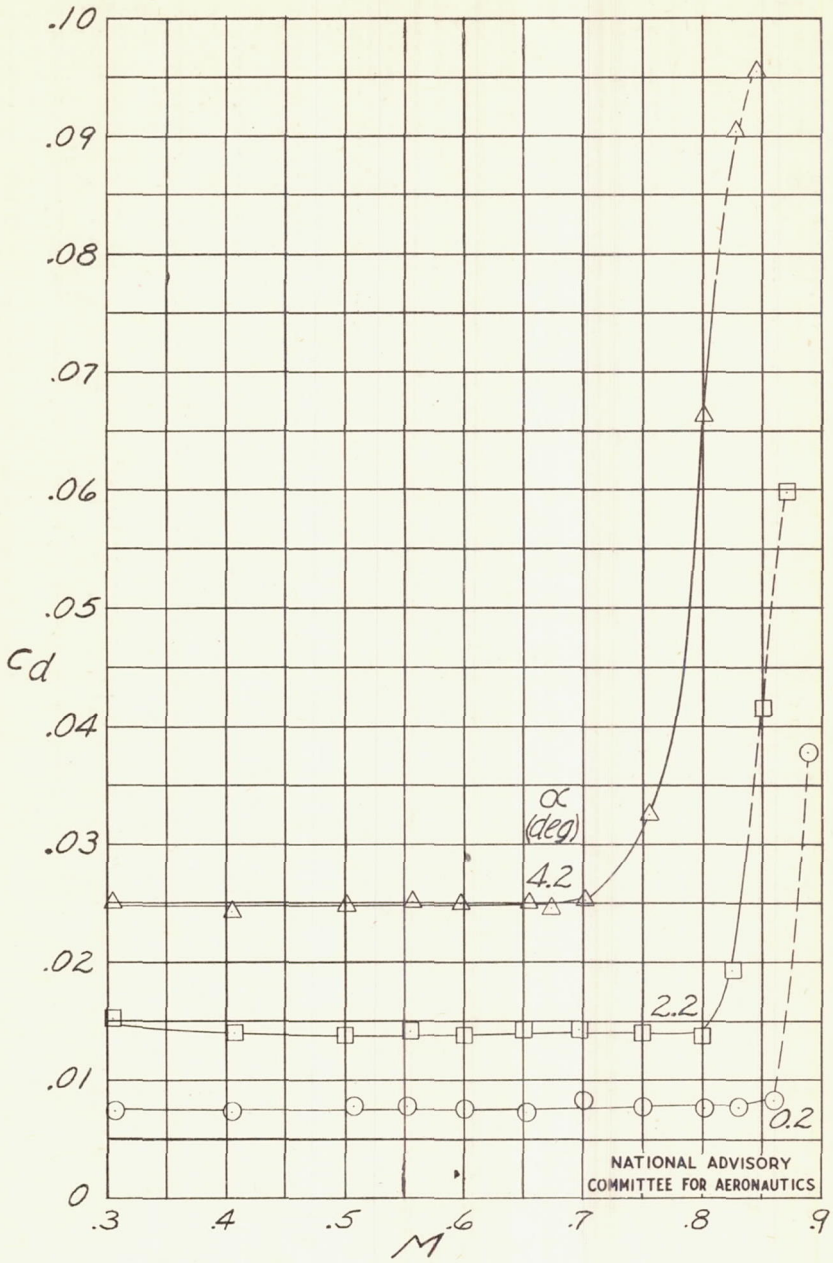

(b) NACA 66-006 airfoil.

Figure 6.- Continued.

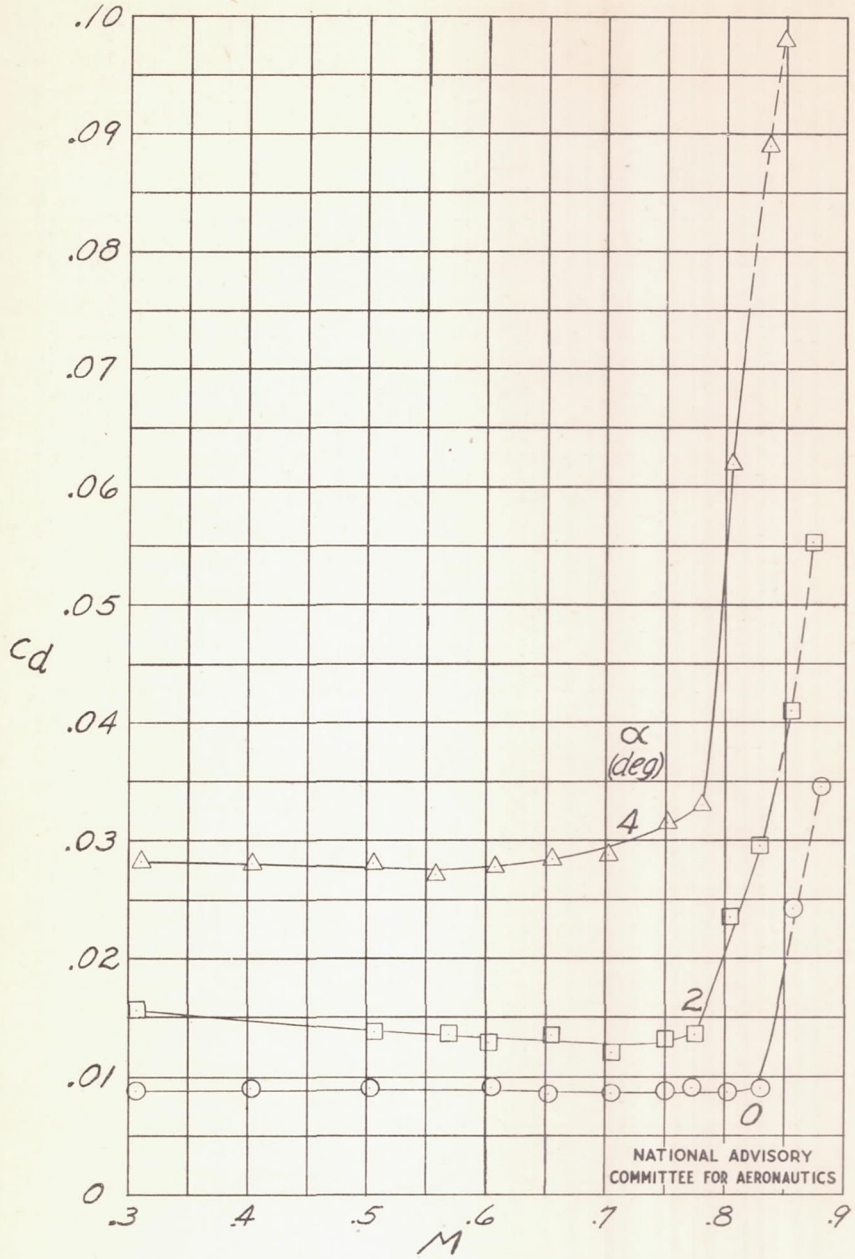

(c) NACA 2S-(30)(03)-(30)(03) airfoil.

Figure 6.- Continued.

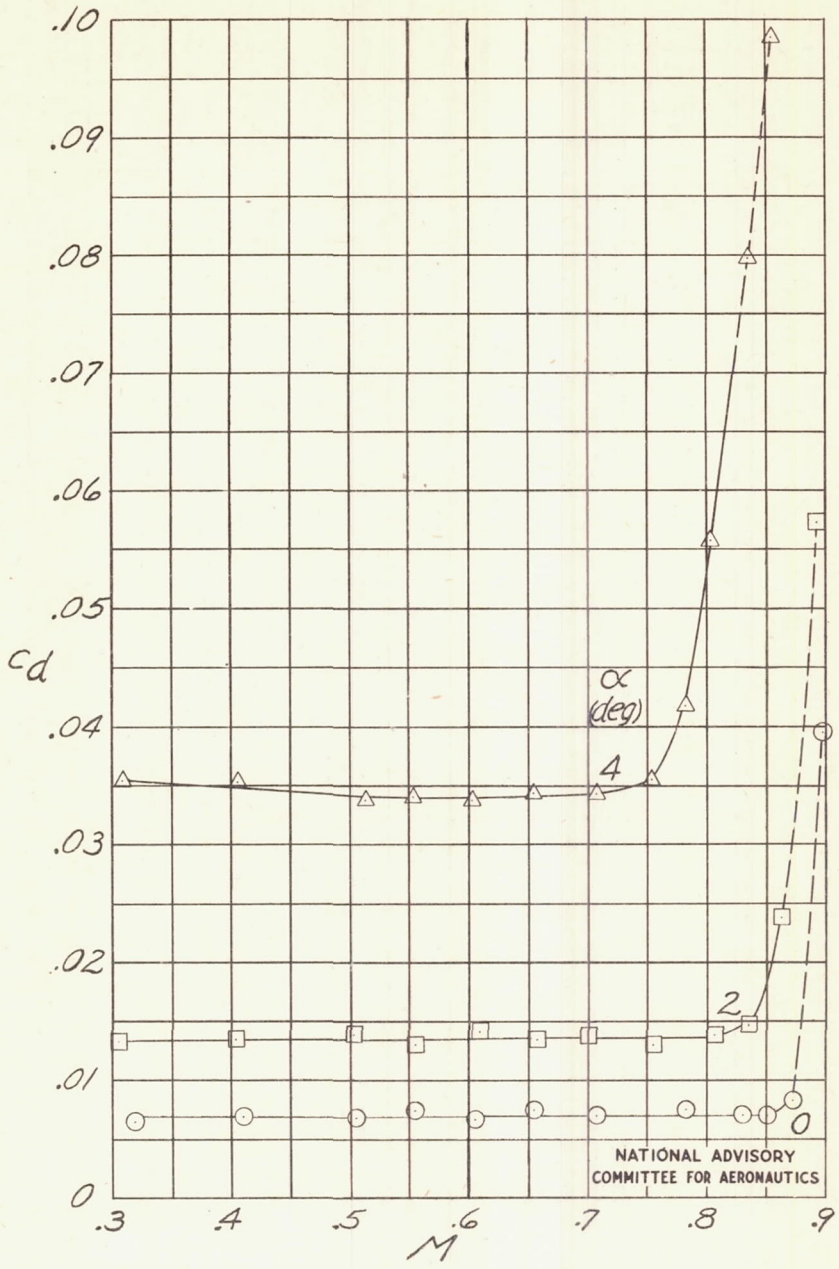

(d) NACA 2S-(50)(03)-(50)(03) airfoil.

Figure 6.- Continued.

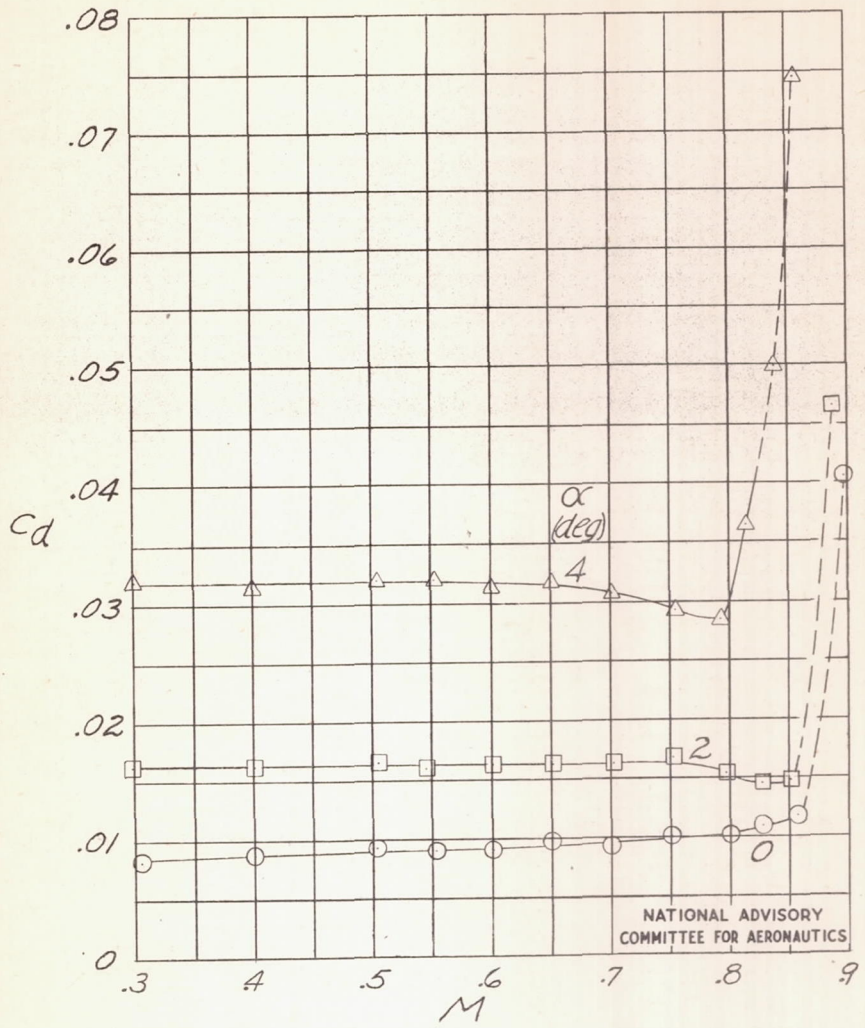

(e) NACA 25-(70)(03)-(70)(03) airfoil.

Figure 6.- Continued.

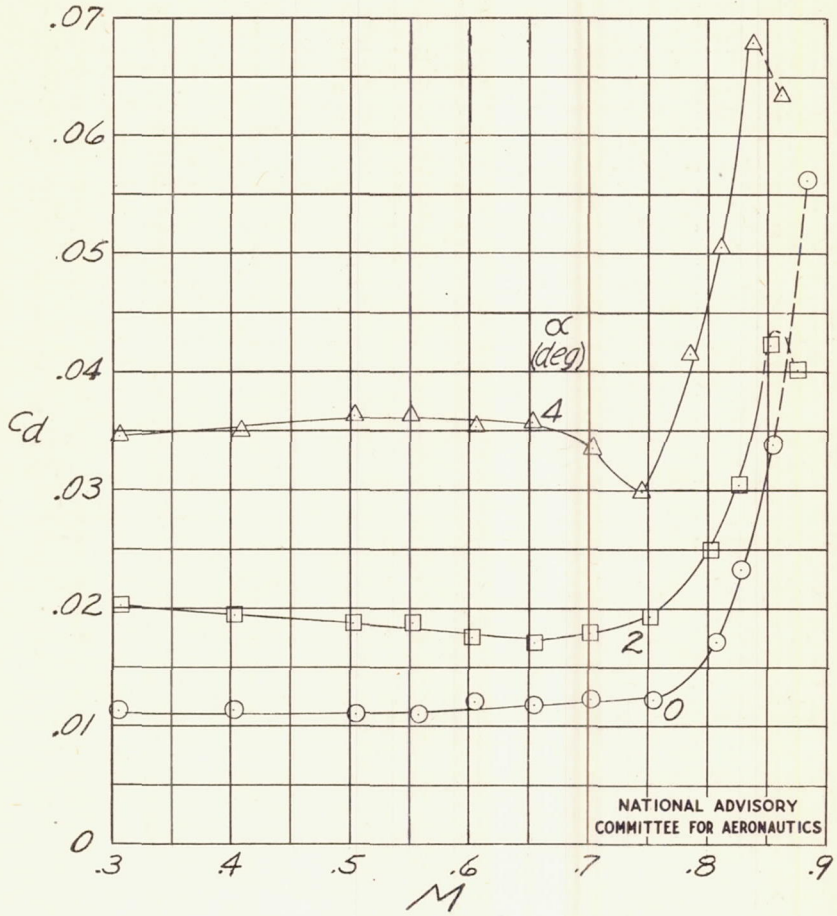

(f) NACA 1S-(30)(03)-(30)(03) airfoil.

Figure 6.-Continued.

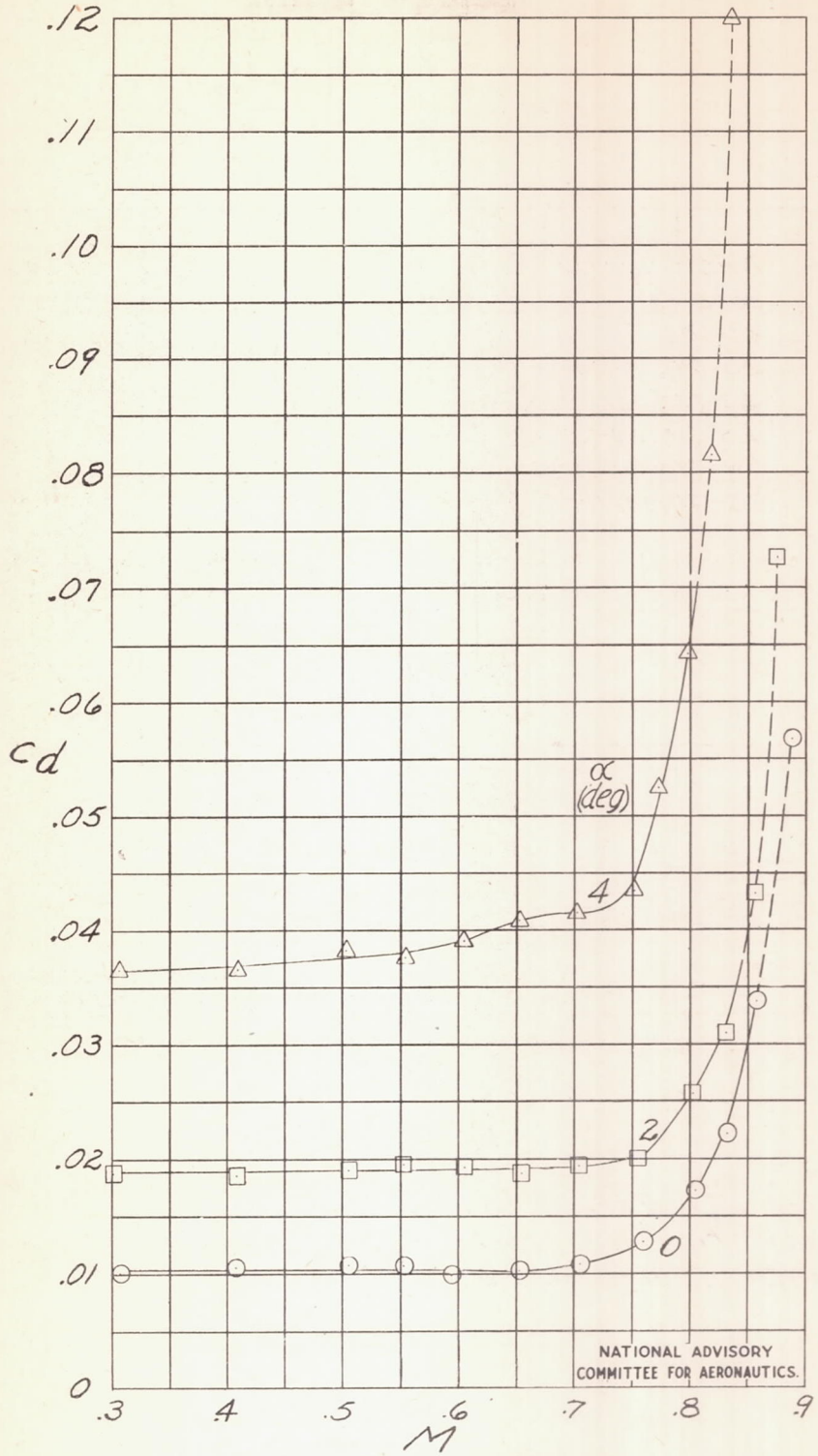

(g) NACA 1S-(70)(03)-(70)(03) airfoil.

Figure 6.- Concluded.

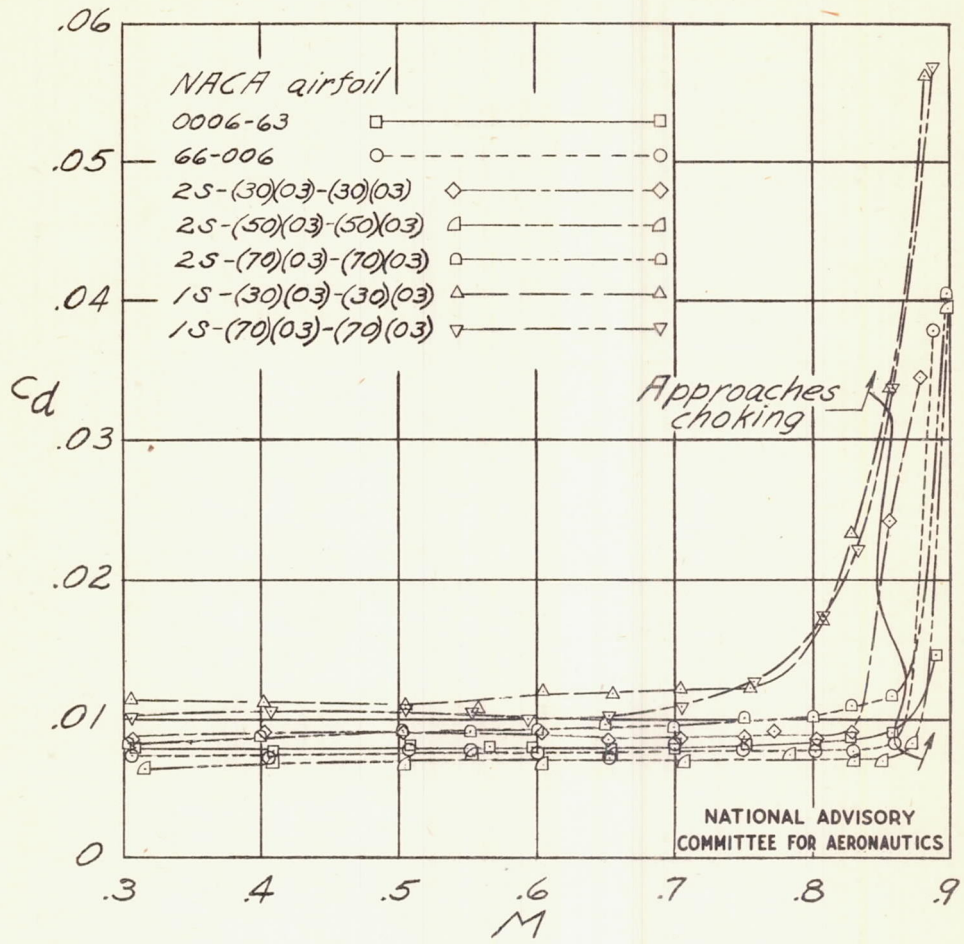

(a) $\alpha = 0°$.

Figure 7.- Effect of airfoil shape on the variation of section drag coefficient c_d with Mach number M.

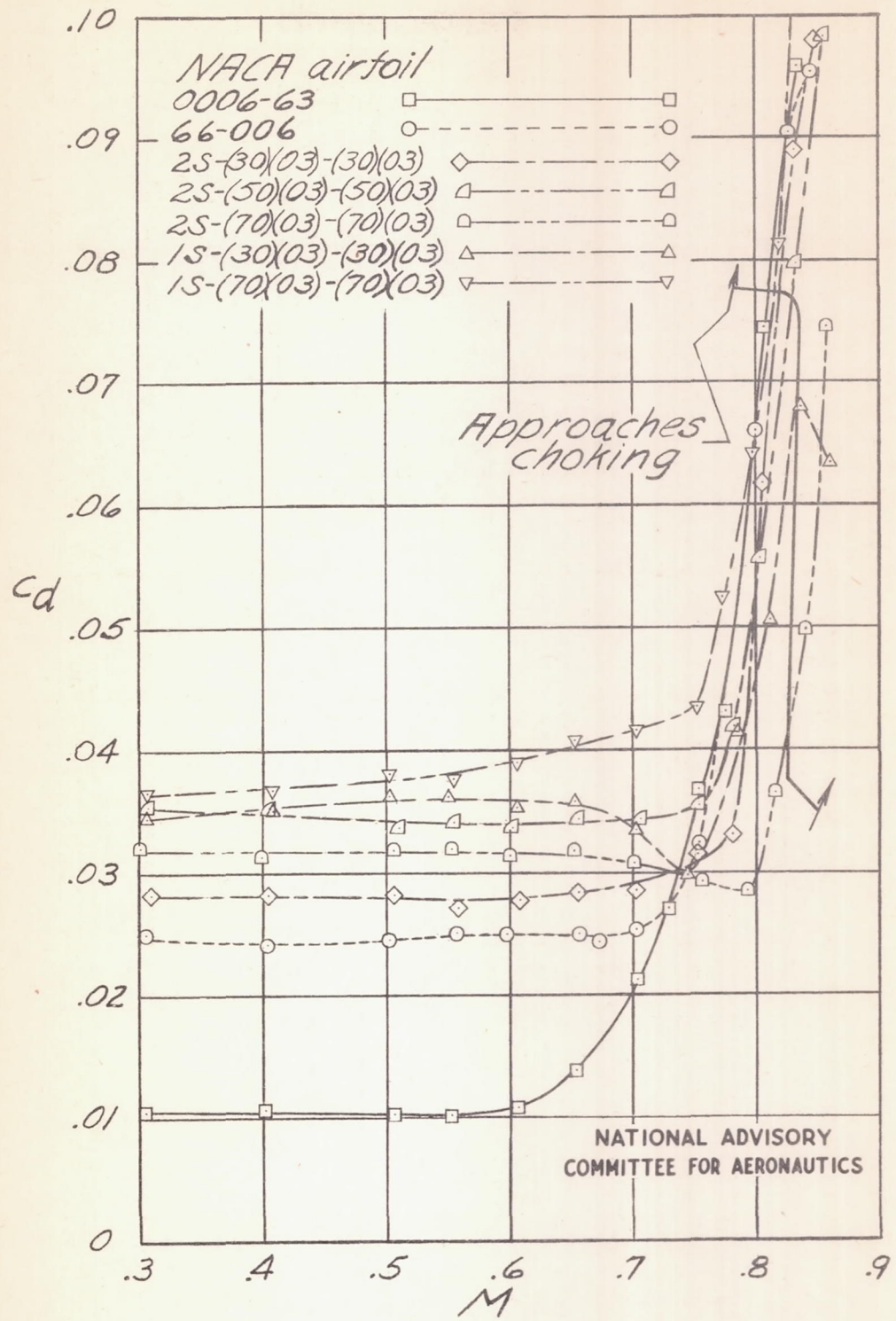

(b) $\alpha = 4°$.

Figure 7.— Concluded.

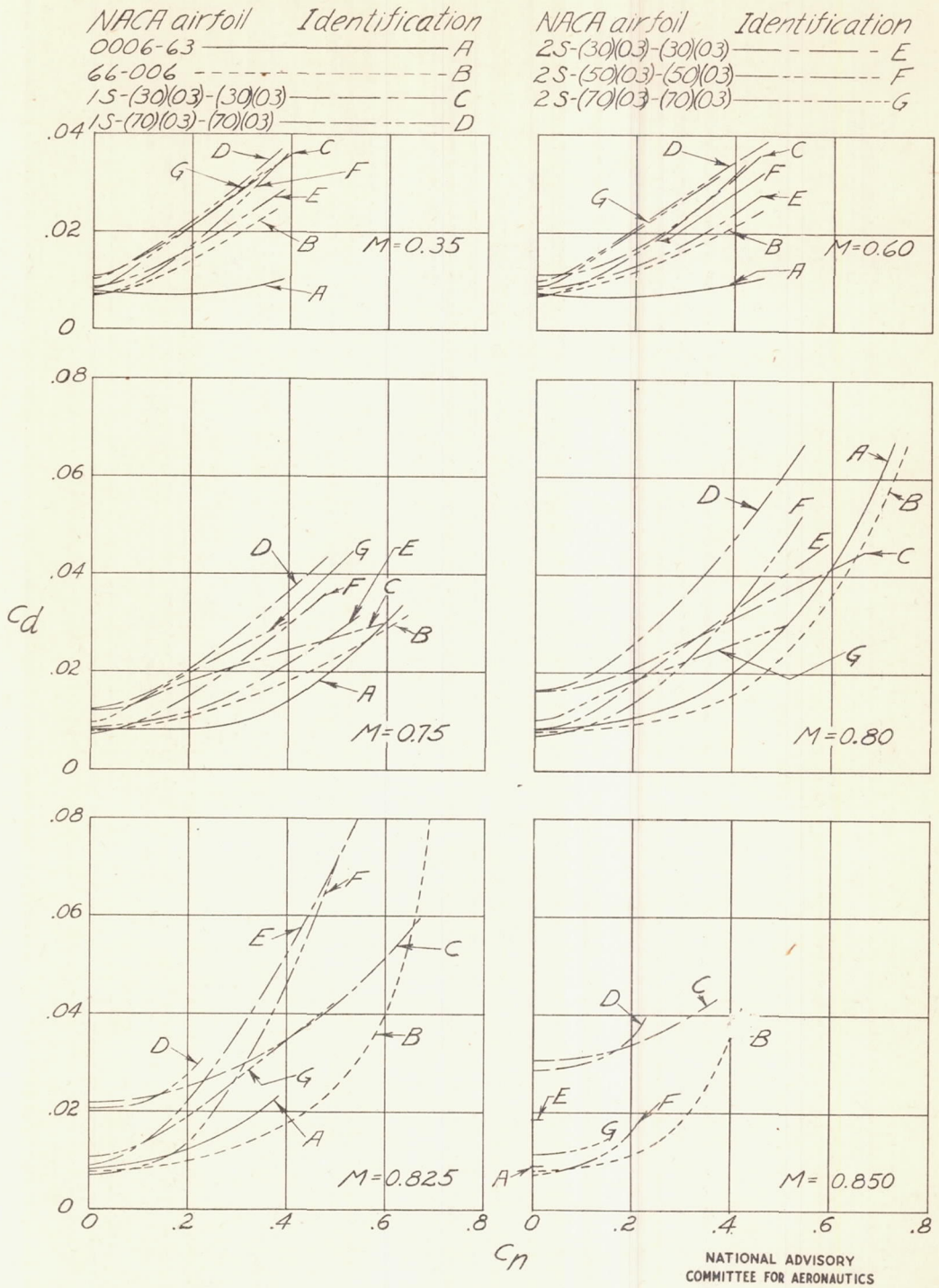

Figure 8.—Effect of airfoil shape on the variation of section drag coefficient c_d with section normal-force coefficient c_n.

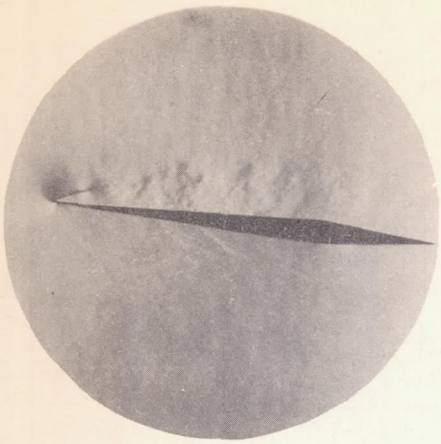

(a) M = 0.50.

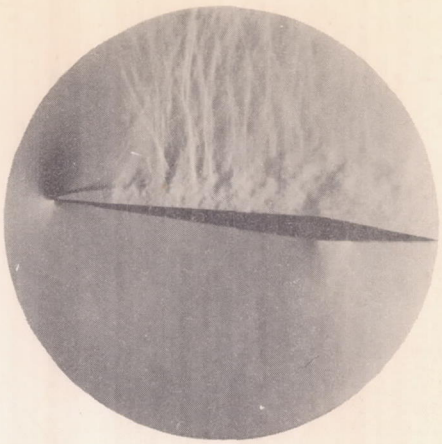

(b) M = 0.70.

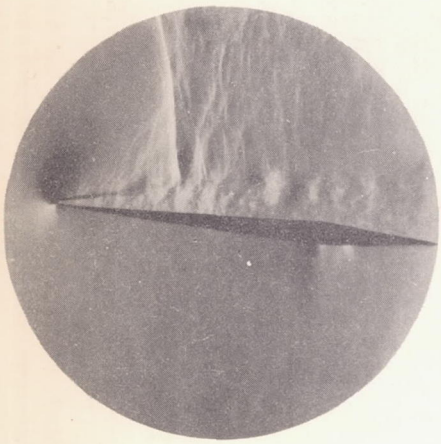

(c) M = 0.72.

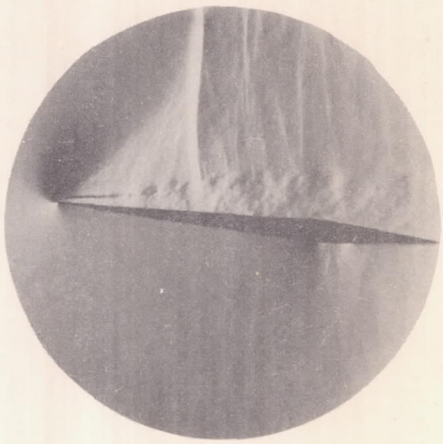

(d) M = 0.75.

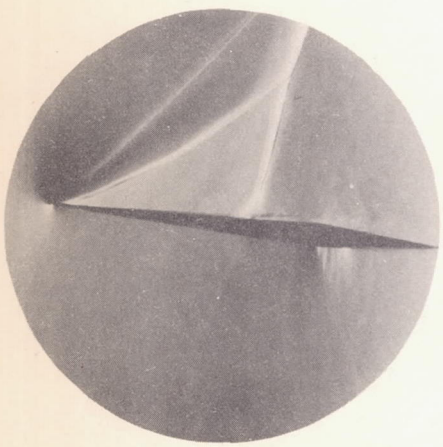

(e) M = 0.77.

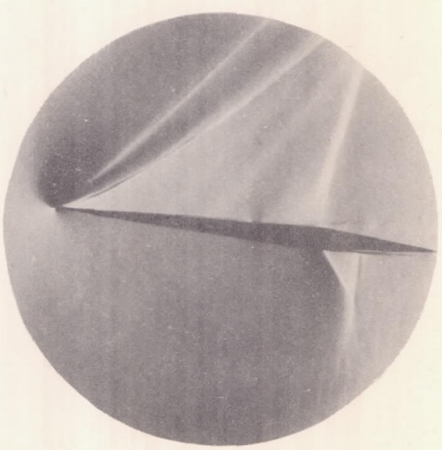

(f) M = 0.80.

Figure 9.- Development of flow phenomena.

NACA 1S-(70)(03)-(70)(03). α = 5.5°.

NATIONAL ADVISORY COMMITTEE FOR AERONAUTICS
LANGLEY MEMORIAL AERONAUTICAL LABORATORY – LANGLEY FIELD, VA.

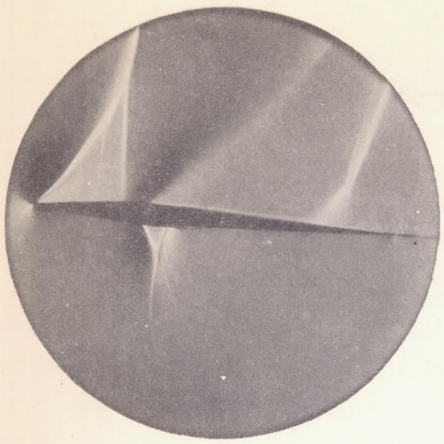

NACA 1S-(30)(03)-(30)(03)

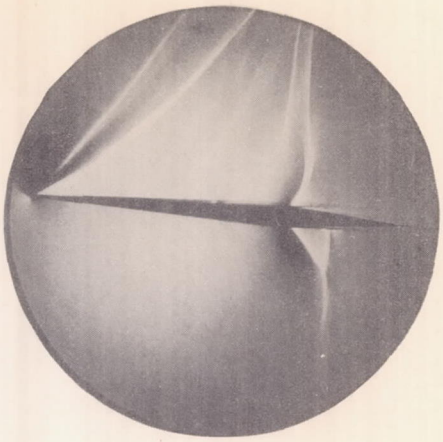

NACA 1S-(70)(03)-(70)(03)

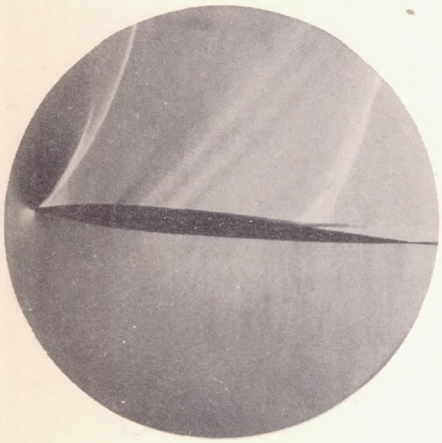

NACA 2S-(30)(03)-(30)(03)

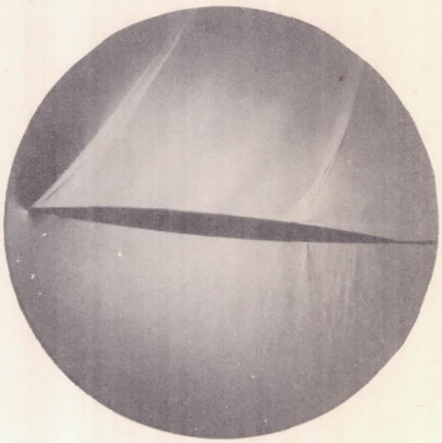

NACA 2S-(50)(03)-(50)(03)

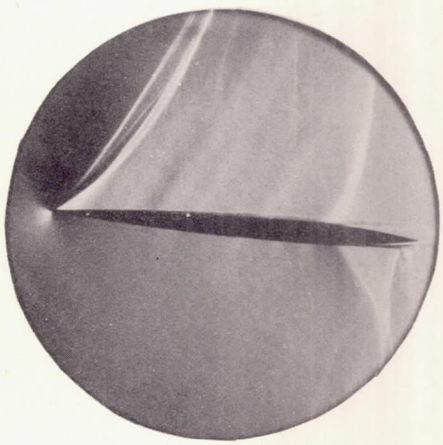

NACA 2S-(70)(03)-(70)(03)

Figure 10.- Flow phenomena on various supersonic profiles.

$\alpha = 4^{\circ}$; M = 0.83.

NATIONAL ADVISORY COMMITTEE FOR AERONAUTICS
LANGLEY MEMORIAL AERONAUTICAL LABORATORY - LANGLEY FIELD, VA.

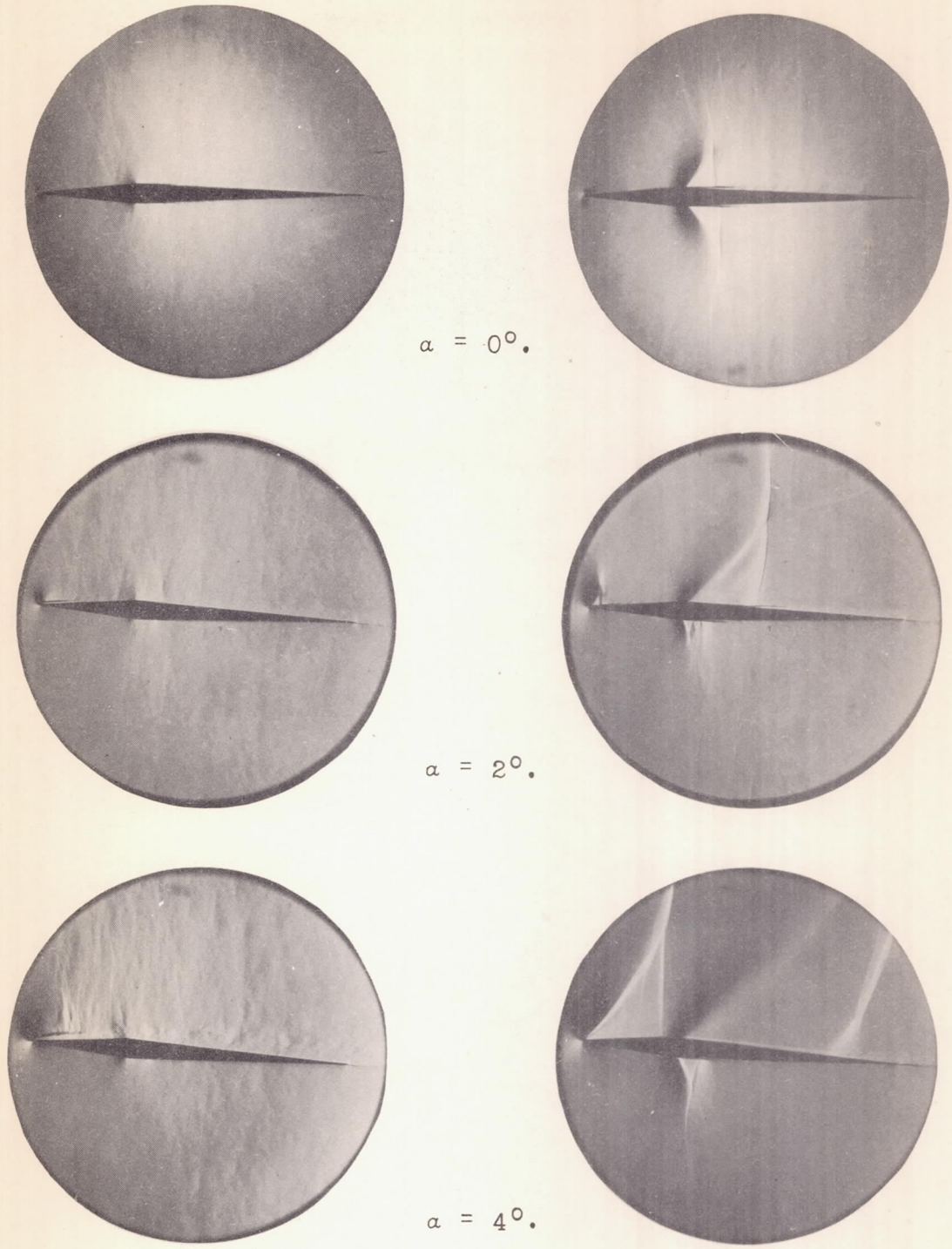

(a) M = 0.65. (b) M = 0.83.

Figure 11.- Variation of flow phenomena with angle of attack. NACA 1S-(30)(03)-(30)(03) airfoil.

NATIONAL ADVISORY COMMITTEE FOR AERONAUTICS
LANGLEY MEMORIAL AERONAUTICAL LABORATORY - LANGLEY FIELD, VA.

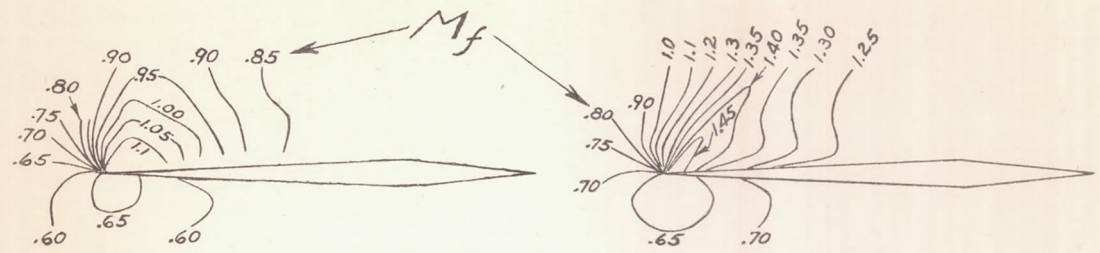

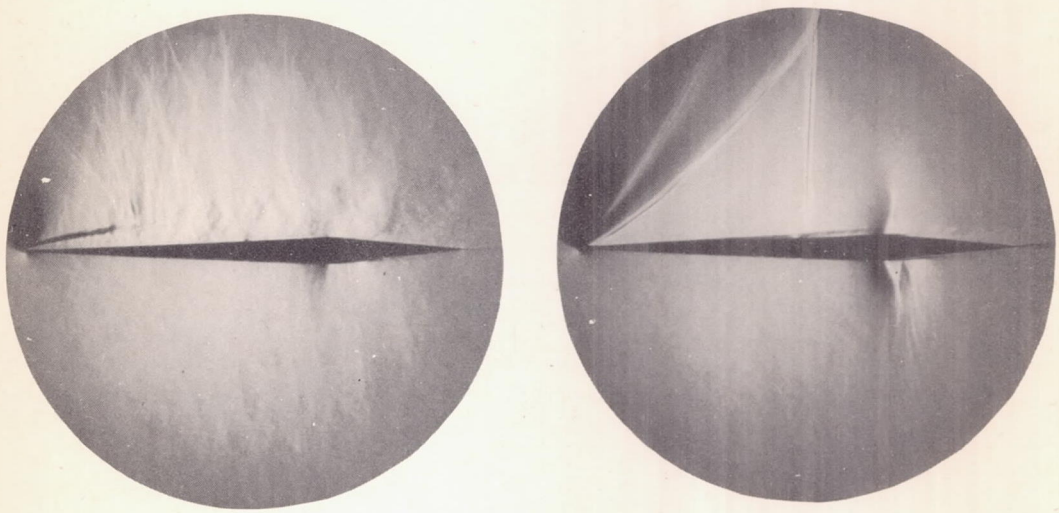

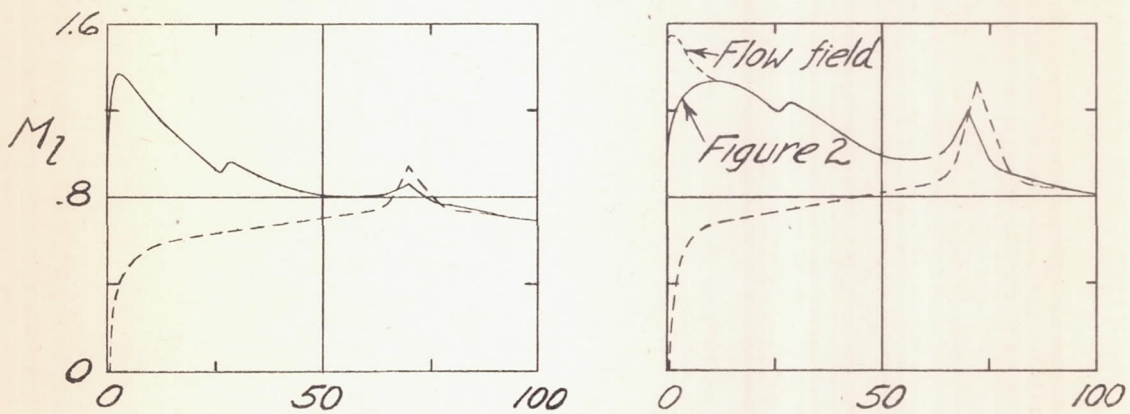

(a) NACA 15-(70)(03)-(70)(03) airfoil; $\alpha = 4°$.

Figure 12.-Details of flow phenomenon.

NATIONAL ADVISORY
COMMITTEE FOR AERONAUTICS

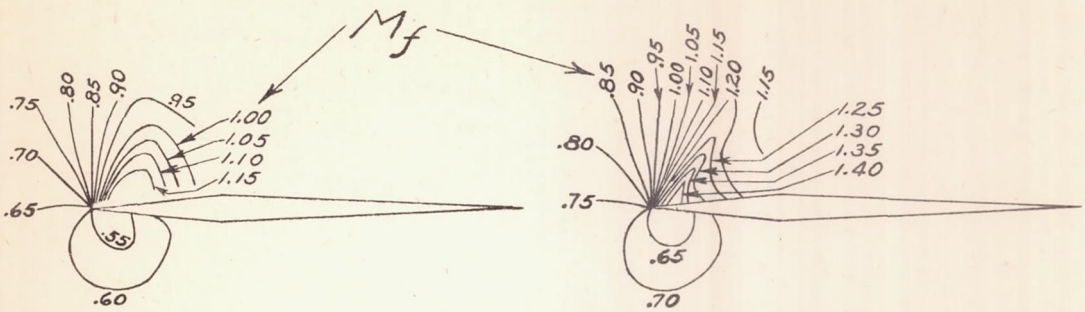

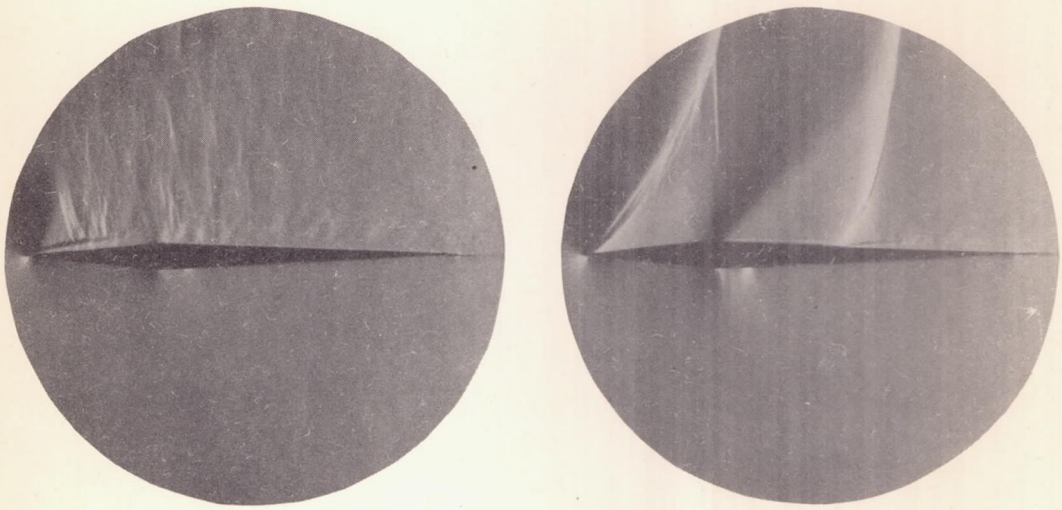

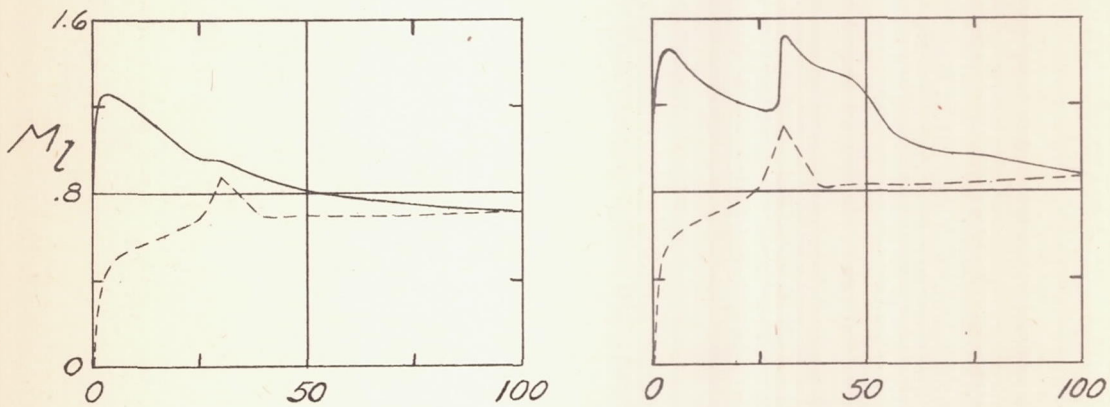

Chordwise station, percent c

M=0.70 M=0.81

(b) NACA 1S-(30)(03)-(30)(03) airfoil; $\alpha = 4°$

Figure 12.- Continued.

NATIONAL ADVISORY
COMMITTEE FOR AERONAUTICS

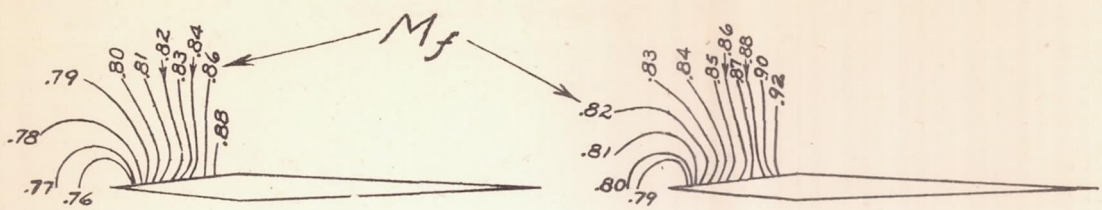

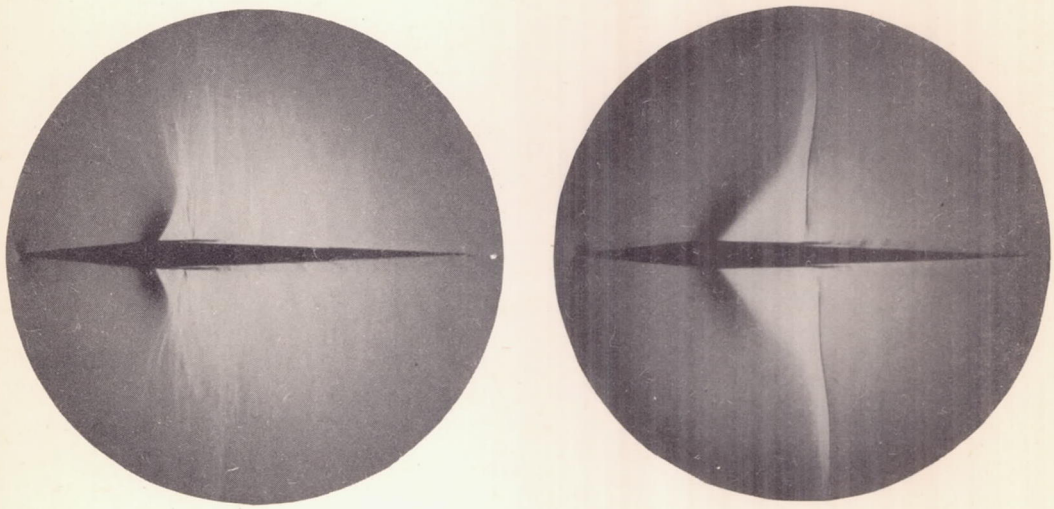

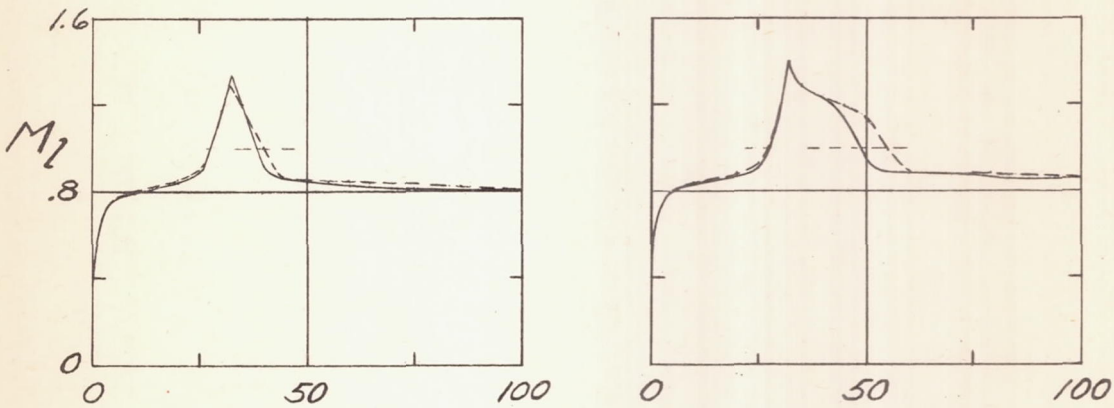

(c) NACA 1S-(30)(03)-(30)(03) airfoil; $\alpha = 0°$

Figure 12.- Concluded.

NATIONAL ADVISORY
COMMITTEE FOR AERONAUTICS

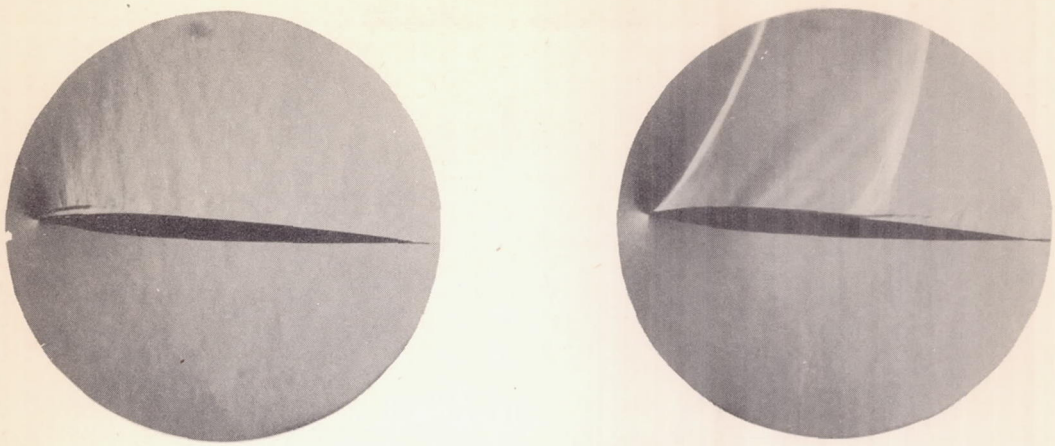

NACA 2S-(30)(03)-(30)(03)

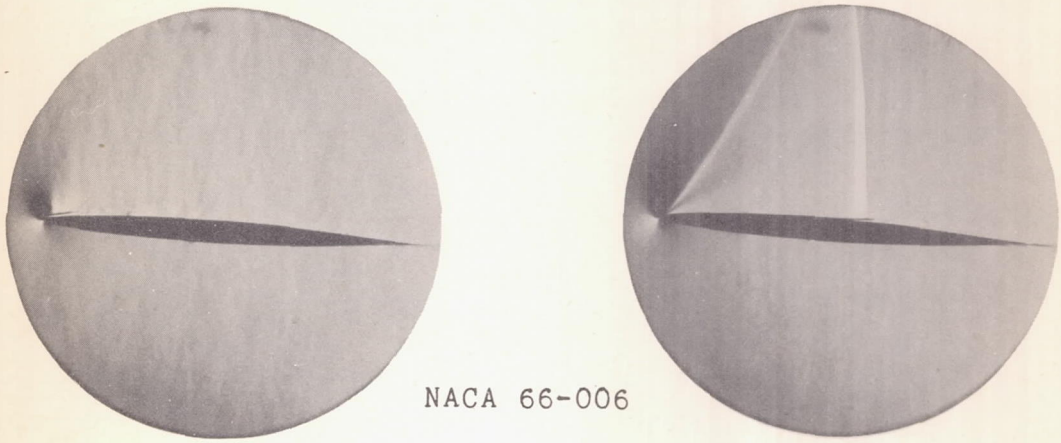

NACA 66-006

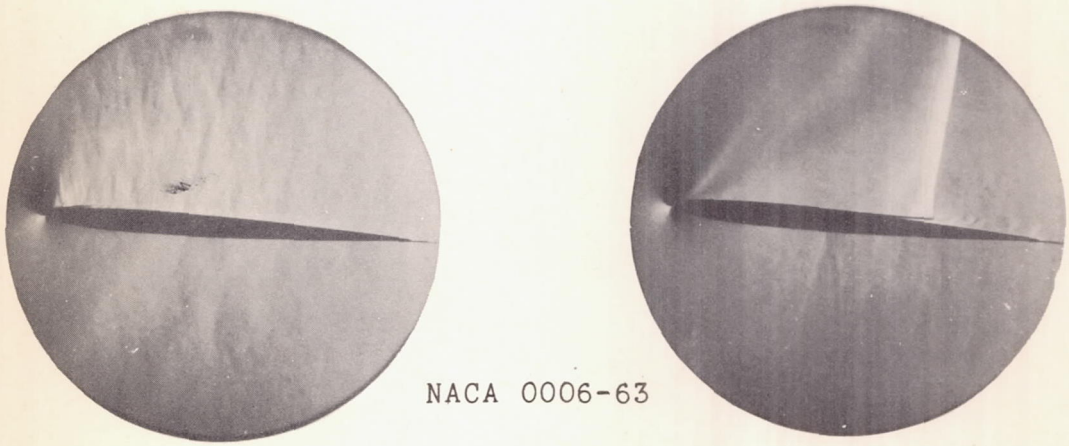

NACA 0006-63

(a) M = 0.60. (b) M = 0.80.

Figure 13.- Effect of leading-edge profile on flow phenomena.

$\alpha = 4^{\circ}$.

NATIONAL ADVISORY COMMITTEE FOR AERONAUTICS
LANGLEY MEMORIAL AERONAUTICAL LABORATORY - LANGLEY FIELD, VA.